Project Number: KLB-0602

DESIGN OF A REPRODUCIBLE MURINE FEMORAL FRACTURE DEVICE

A Major Qualifying Project Report:

Submitted to the Faculty

Of the

WORCESTER POLYTECHNIC INSTITUTE

In partial fulfillment of the requirements for the

Degree of Bachelor of Science

By

_____

_____

_____

Melissa A. Byrne
Benjamin C. Cleveland
Joseph E. Marturano

Date: March 1st, 2007

Approved:

_____
Prof. Kristen L. Billiar, Major Advisor

1. fracture mechanics
2. biomechanics
3. mouse
4. bone

_____
John J. Wixted, MD, Co-Advisor

TABLE OF CONTENTS

ACKNOWLEDGEMENTS

ABSTRACT

Mouse models are commonly used to investigate bone healing and test new treatments. The objectives of this project were to design a fracture device to create a reproducible transverse fracture in the mouse femur and to establish the limits of achieving transverse fractures. Testing with 26.4±6.1g wildtype mice (n=120) developed a model equation of $mv^2 = 0.292$ to predict a 95% transverse fracture success rate. These results are useful to researchers who are interested in obtaining a higher transverse fracture success rate.

TABLE OF FIGURES

TABLE OF TABLES

1. INTRODUCTION

Bone fractures are an important societal concern because sustaining one is painful, debilitating and results in lost productivity from time spent healing instead of working. Previously, healing a bone fracture took an external approach, and relied on casts, bone plates and screws to fixate the fracture and let the body heal itself. But a newer, more internal approach is necessary to expedite fracture healing using modifications on a cellular level. One theorized mechanic to assist bone healing is the role of leukotrienes in fracture response and whether or not blocking these lipid mediators may reduce healing time. Studying mouse models in orthopaedic research from this cellular perspective, which has seen a rise in popularity in recent years (Carmouche et al., 2005), may lead to advances in fracture recovery time from genetic similarities between mice and humans.

Despite enthusiasm from orthopaedic surgeons and researchers, many of the previously designed fracture devices have not created completely reproducible fractures or have relied on very slow loading techniques that are not representative of most injuries (Manigrasso & O'Connor, 2004). This results in either discarded mice or uncertainty with degree of soft-tissue damage in the fracture. Ideally a mouse femur fracture model would produce viable data in each experiment, increasing overall efficiency.

The ideal fracture type for mouse models is a transverse fracture while avoiding open, oblique or comminuted fractures.   A comprehensive bone fracture study by McGee, Qureshi and Porter (2004) demonstrated that the two primary factors in producing a transverse fracture were small load area and low kinetic energy. In addition, it is desirable to create soft tissue damage in an impact to simulate the effect of

1

mesenchymal stem cell activity and inflammation response that occur in most high-energy fractures (Minguell et al, 2001; Boyan et al, 1999). Through understanding of these bone fracture factors, it is possible to create a device specifically designed to simulate the effect of a high energy impact that may be observed in human bone trauma.

The goal of this project was to design and develop a device to create reproducible fractures for mouse femur bone growth studies. The device was engineered to produce a closed, transverse, diaphyseal fracture using a controlled impact. This would permit the most reproducible measurement of bone re-growth and have a realistic level of soft tissue damage, unlike any other previous devices. In addition, the design incorporated a novel mouse positioning system (MPS) that improves reproducibility by minimizing positioning variability of the femur. It also reduces human error and increases efficiency by using few adjustable factors and enables one-person operation.

A common measure of success used by researchers using previous fracture devices is the percentage of transverse fractures achieved of total attempts. However, it is our desire to develop relationships between mouse weight and kinetic energy at fracture to further the understanding of fracture mechanics. A result of this study is the establishment of kinetic energy limits to increase reproducibility of transverse fractures. The methods and the results in this study are useful in the design of other precision fracture instruments and in future murine bone healing studies.

2. LITERATURE REVIEW

Fracture Healing and Mouse Models

One example of the "new" and currently theoretical method to expedite fracture healing is illustrated using mesenchymal stem cell (MSCs) proliferation pathways as shown in Figure 1. The mechanical stimuli brought on by a fracture and soft tissue damage cause MSCs in the bone marrow and bloodstream to activate an immune response, which is thought to aid in osteogenesis (Tor, 2006).
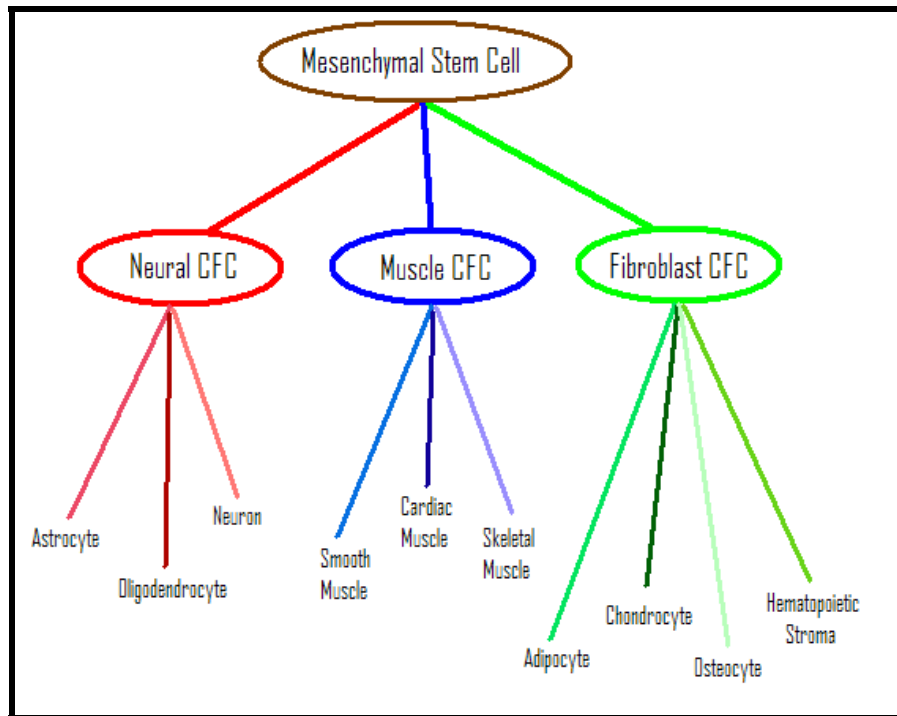
Figure 1: Mesenchymal stem cell proliferation pathways based on Colony Forming Cell (CFC) groups (Tor, 2006)

It is thought that selecting against all pathways except osteocytes may reduce fracture healing time by increasing the efficiency of osteogenesis. Thus one end-goal of

using fracture devices is to use mouse models to determine what drugs can speed the healing process in mice, which may directly translate to faster healing time in humans.
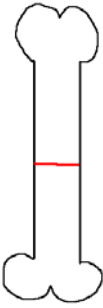
Bone Fracture Mechanics

Introduction and fracture types

All materials will fracture once subjected to a load exceeding a critical strength. The mechanisms for fracture in linear elastic materials such as metals or ceramics are different than in bone for two reasons. First, the anisotropic nature of bone gives rise to different mechanical properties in different loading directions. Cortical bone samples tend to have almost twice the elastic modulus and compressive strength in the axial direction than in the transverse direction (Wirtz et. al, 2000). The second reason is the stiffness of bone increases with increasing strain rate from its viscoelastic properties (Ozkaya and Nordin, 1999). The magnitude of stiffness has a significant role in the end result of fracture. Thus in designing a mouse femur fracture device, the anisotropic and viscoelastic properties of bone must be taken into account in order to create the most reproducible fracture possible.

There are several major types of closed fractures in long cortical bone. The term "closed" in this sense refers to a fracture that has not exposed the bone to the outside environment and has the newly created fracture surfaces remaining in contact. The type of fracture that is created is determined primarily by the three-dimensional stress state on the bone. Table 1 provides a brief summary of the most common fracture types and their general causes.

Table 1: Common fracture types in long bones

Type	Transverse	Oblique	Spiral	Comminuted
Illus.				
Mech. Cause	Bending moment	Bending moment & compression	Torsion	High energy impact

It is important to understand and define these fracture methods because they are not all ideal for bone healing studies. The transverse fracture is the simplest type and is defined as a straight fracture with less than a 30° deviation from the minor axis of a long bone. If the angle exceeds this, it is defined as an oblique fracture (Brainard, Slauterbeck and Benjamin, 1992). A spiral fracture is a helical-shaped crack which is sometimes incorrectly diagnosed as an oblique fracture. Finally a comminuted fracture is a transverse fracture which has separated and caused multiple fracture paths. This type typically creates many bone fragments and is difficult to heal and characterize.

The common element between the fractures is that in each case an external stimulus generated enough "force" to propagate the crack. There are many different means for applying a loading state to a bone. Perhaps the most common experimental method to apply a load is three-point bending, wherein the desired sample is suspended in the air by its two ends and a load is applied to the middle. Torsion is another method, where the two ends of a bone are rotated in opposite directions relative to each other. There is also tension and compression, which involve the direct "pulling" or "pushing" of

a material, respectively. Note that in each of these cases, the strain rate is considered to be small. However another possibility exists, where the load is applied very rapidly. This final stress condition is referred to as "impact" and is very important in biological fracture mechanics. These loading states form one part of the overall determination of the type of break from a given stress state.

There are also several means to apply an impact load to bone. The most commonly used today is gravity, wherein a weight is dropped and accelerated to a certain velocity to drive a crack through the whole bone diameter. Another common method is a pneumatic device which uses air pressure to drive a shaft into the bone. This means of crack propagation was one of the first ever used on rats or mice (Jackson et. al, 1970). A solenoid assembly could also be used to fracture bone. In this case, magnetic force from an electromagnet would drive a magnetic shaft through an enclosed cylinder into the bone. One final method could be a partial cam system that would extend an arm on a rotating wheel forward into the bone; this is typically reserved for cyclic applications but can be adapted for fracture purposes.

It is therefore clear that there are a wide variety of fracture types along with even more means to apply a loading state and generate a load. Choosing the correct parameters for the purposes of a mouse femur fracture experiment requires careful consideration of the desired goal. The most common means of measuring bone growth is through the use of radiography. While developing an x-ray is not very complex, measuring the rate of bone growth can be if the fracture is not the correct type. Several researchers feel that the easiest and most precise method of bone growth measurement occurs when the fracture is transverse with minimal fragments (Bonnarens and Einhorn,

1984; Yaoita et. al, 2000). Thus, creating transverse fractures while avoiding other types

will enable the most accurate assessment of bone growth. The location of the fracture is

also important for reproducibility and consistency of fracture type. The fracture should

occur in the middle-third diaphysis of the femur to ensure fracture of cortical bone.

Fracture theory

While it is apparent that a transverse fracture is the most ideal type, the method to

create one is less clear. In order to understand how to best reproduce a transverse

fracture, one must first analyze the mechanics of a fracture and the factors that affect it.

This analysis is provided below, starting with crack propagation from a theoretical aspect

and moving into fracture factors such as kinetic energy, stress waves, positioning and

soft-tissue damage.

The study of fracture mechanics originated with Griffith's World War I research

in failure of brittle materials (Griffith, 1920). He determined that a certain surface energy

is necessary to propagate a crack and drive two surfaces apart. This energy must be in

proportion to the elastic strain energy released from separation (Perez, 2004). One

method to generate surface energy is through application of stress states, typically tensile

stresses. The characteristics of fracture through stresses have been thoroughly

characterized by Irwin and Orowan shortly after Griffith's work. Another method to

create surface energy is to generate potential and kinetic energy from an impact to break

apart molecular bonds in the material to extend a crack (Martin, Burr and Sharkey, 1998).

The relationship between energy and crack propagation may be explained by the

energy principle approach, which takes into account mechanical work, energy absorption

around the crack tip and expended heat (Perez, 2004). To summarize, this states that

fracture will occur when the supplied energy exceeds the resistance of the material, provided that plastic deformation and heat dissipation are also taken into account. In other words, there is a certain level of strain energy that would be released if two areas of material were separated and the applied energy must equal it, from the First Law of Thermodynamics. This relationship, known as the "Griffith energy balance", may be written as:

$$\frac{dE}{dA} = \frac{dU}{dA} + \frac{dW_S}{dA} = 0$$

Where dA is the crack area, U is potential energy (supplied by external forces and internal strain energy) and W_S is the work required to create new surfaces (Anderson, 2005). It therefore follows that:

$$-\frac{dU}{dA} = \frac{dW_S}{dA}$$

Thus, the supplied potential energy must equal the strain energy required to separate the surfaces and propagate the crack. It is useful to take into account applied potential and kinetic energies into a fracture device. For the gravity driven example described earlier, this would correlate to the mass and velocity of the striker.

The importance of 3D femur positioning

One goal described earlier was to avoid oblique fractures (>30° deviation from minor axis) and only obtain transverse fractures. A propagating crack does not necessarily have to stay in its initial plane; research has shown that cracks will either seek the path of least resistance or the plane of maximum force (Anderson, 2005). Thus, the orientation of applied energy is very important in the final direction of the crack. In bone fracture, the path of least resistance is in the transverse direction (normal to the long axis)

8

due to its anisotropic nature - cortical bone (the target in this study) shows approximately a 40% decrease in fracture toughness in directions perpendicular to its long axis (Nalla, Kinney and Ritchie, 2003). Thus, provided that the plane of maximum force is also in the transverse direction, a transverse crack should propagate with minimal angular displacement, as shown in Figure 2. This is also under the assumption of low kinetic energy to minimize the effect of stress waves, which will be described in detail later. Therefore an effective means to avoid oblique fracture is to ensure the plane of maximum force is normal to the long axis of the bone. In Figure 2, this would correspond to the alignment of the blue dashed line (path of least resistance, the minor axis) and the green dashed line (plane of applied energy or force).
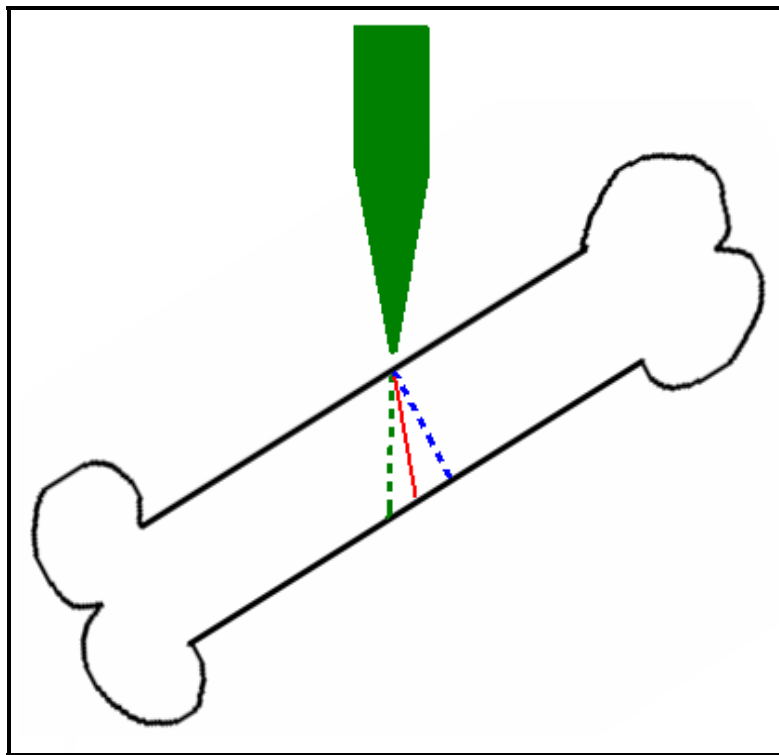
Figure 2: A crack will propagate between the plane of maximum force and the path of least resistance; green dotted line represents plane of maximum force, blue transverse line is path of least resistance and red line is the actual fracture result; figure is a visual representation of the importance of aligning the striker (plane of maximum force) in the transverse direction (path of least resistance)

The importance of kinetic energy

The other desirable goal described previously was to avoid comminuted fractures (fragments) and only obtain transverse fractures in the mouse femurs. For the case of bone, it has been determined that the relationship between kinetic energy ($E_K = \frac{1}{2}mv^2$) and comminuted fracture occurrence is proportional – the higher the kinetic energy, the greater the chance of comminuted fracture (Martin, Burr and Sharkey, 1998). There are two central reasons for this, as described below.

First, research by Mott (1948) has shown that there is a relationship between kinetic energy and speed of crack propagation, both in the speed of the surface separation and stress waves, as shown in the following equation:

$$V = \sqrt{\frac{(2k)E_k E^2}{\rho a^2 \sigma^2}}$$

V = Speed of crack
k = constant
E_k = kinetic energy
E = elastic modulus
ρ = mass density of material
α^2 = crack length
σ = amplitude of stress wave

Thus, as kinetic energy increases, the speed of crack propagation increases. Under dynamic loading, a slow crack provides enough time for material adjacent to the crack to become unloaded, which arrests crack formation in the nearby area of the crack (Martin, Burr and Sharkey, 1998). However, with increasing kinetic energy, stress waves result from the faster crack velocity, whose speed approaches sound waves for one-dimensional wave propagation (Anderson, 2005). This speed is so fast that the material does not have enough time to adjust and arrest crack propagation, resulting in fracture at multiple sites. The end result is a fragmented, comminuted fracture as shown in Figure 3.
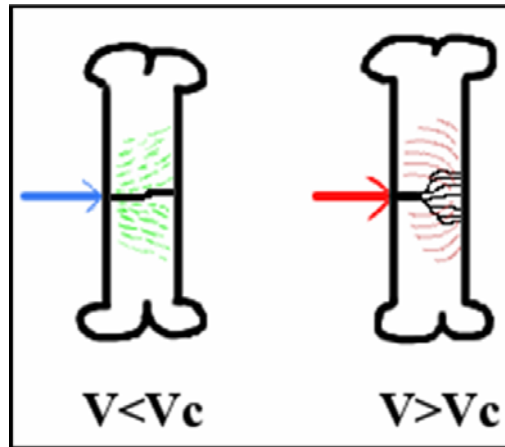
Figure 3: Crack propagation velocity beyond a critical value will result in stress waves and comminuted fracture

Secondly, the fact that higher kinetic energy results in an increased rate of comminuted fractures is also related to crack velocity equation. In most materials, the elastic modulus is constant; however this is not the case in bone. Since bone is viscoelastic, its elastic modulus increases with increasing loading rate (Ozkaya and Nordin, 1999). Thus, the higher velocity the bone is impacted with, the higher the stiffness it will have. If stiffness increases, the speed of the stress wave increases as well from the above equation. The viscoelastic properties of bone augment the relationship between increasing kinetic energy and likelihood of comminuted fracture.

It is therefore clear that reducing kinetic energy, especially velocity of impact, will reduce chance of comminuted fracture. This relationship has been shown experimentally as well: a comprehensive bone fracture study by McGee, Qureshi and Porter (2004) demonstrated that the primary factors in producing a transverse fracture were low kinetic energy and a small load area.

Energy and soft-tissue damage

A final consideration for the most ideal fracture type is degree of soft-tissue damage. While slow three-point bending will eventually fracture a bone, this is an atypical fracture in practice. Everyday fractures in healthy individuals occur mostly from highly dynamic impacts, such as automotive accidents or sports injuries (personal communication, J. Wixted MD, 2006). These fractures have a moderate to high level of soft-tissue damage associated with them. Therefore to accurately reproduce a fracture that an individual might experience, soft-tissue damage should be created. In addition, soft-tissue damage is necessary for the dispatch of MSCs for osteogenesis to the fracture site (Minguell et. al, 2001; Boyan et. al, 1999).

The degree of soft-tissue damage is dependant on kinetic energy of the impact. A study on the effect of an aluminum hammer impact on the cranium noted that the magnitude of energy absorbed per area of the tissue was directly proportional to the level of blood flow loss, necrosis of adipose tissue, loss of muscle tissue, level of bacterial infection and inflammation severity (Cardany et. al, 1976). Similarly, a finite element study of drop weight impacts on pig kidneys demonstrated that rupture was not dependant on rate or mass, but was dependent on the combination of the two (Snedeker et. al, 2005). Therefore soft-tissue damage is necessary for full realization of the study and the governing mechanical relationship of soft tissue damage is kinetic energy.

Summary of fracture mechanics and soft-tissue damage

At this point it is seen that a certain level of kinetic energy is necessary for soft-tissue damage, but that kinetic energy must be minimized to avoid comminuted fracture. Therefore, the ideal kinetic energy at impact should be just under the threshold of

12

comminuted fracture in order to obtain a transverse fracture and elicit maximum MSC response. This continuum relationship is represented below in Figure 4.
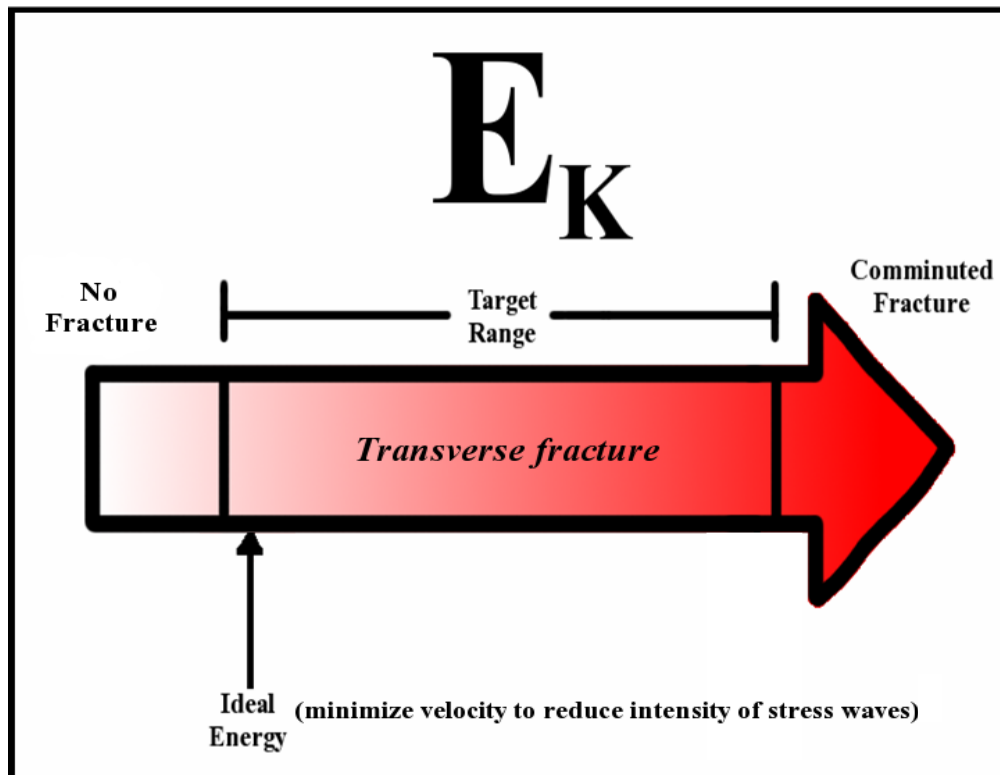
Figure 4: Schematic illustration of kinetic energy continuum in impact model; ideal level of kinetic energy is just above the threshold past no fracture to reduce velocity of stress waves

The study of fracture mechanics can provide insight into the best methods to produce the desired fracture and soft-tissue damage. There are several fracture types and means to create a fracture. A transverse fracture, where the bone crack has less than a 30° deviation from the minor axis, is the most desirable due to ease of measurement with radiography. To create the fracture, it was shown that kinetic energy is the fundamental mechanical consideration and that there were three potential problems that could arise during the fracture. From analyzing the theory of fracture, bone fracture studies and impact research, the following solutions to these problems were obtained:

1. Comminuted fracture – prevent by reducing kinetic energy of impact

2. Oblique fracture – prevent by ensuring that impact is perpendicular to long axis

3. Low soft tissue damage – prevent by increasing kinetic energy of impact, but not past the threshold into comminuted fracture

The application of these solutions to a fracture device will increase the reproducibility of a transverse fracture with soft-tissue damage. This will minimize the number of discarded mice from improper fractures.

Prior Mouse Femur Fracture Devices

In the past, several different femur fracture devices have been created. The first device, and what most current devices have been modeled from, is the Bonnarens and Einhorn design. This study's device used three point bending with the leg of the mouse suspended on top of two anvils. A blunt tipped guillotine striker is then lowered onto the femur using a force generated by gravity (1984). Einhorn's model can be seen in Figure 5. Another famous study is the Jackson study, which developed the idea of only allowing the striker to deflect the top of the femur a distance equal to half the diameter of the bone, as seen in Figure 6. However, in the Jackson model, the fracture was achieved by using compressed air at 40psi. This method was found to be inconvenient due to frequent replacement of compressed air supply tanks.
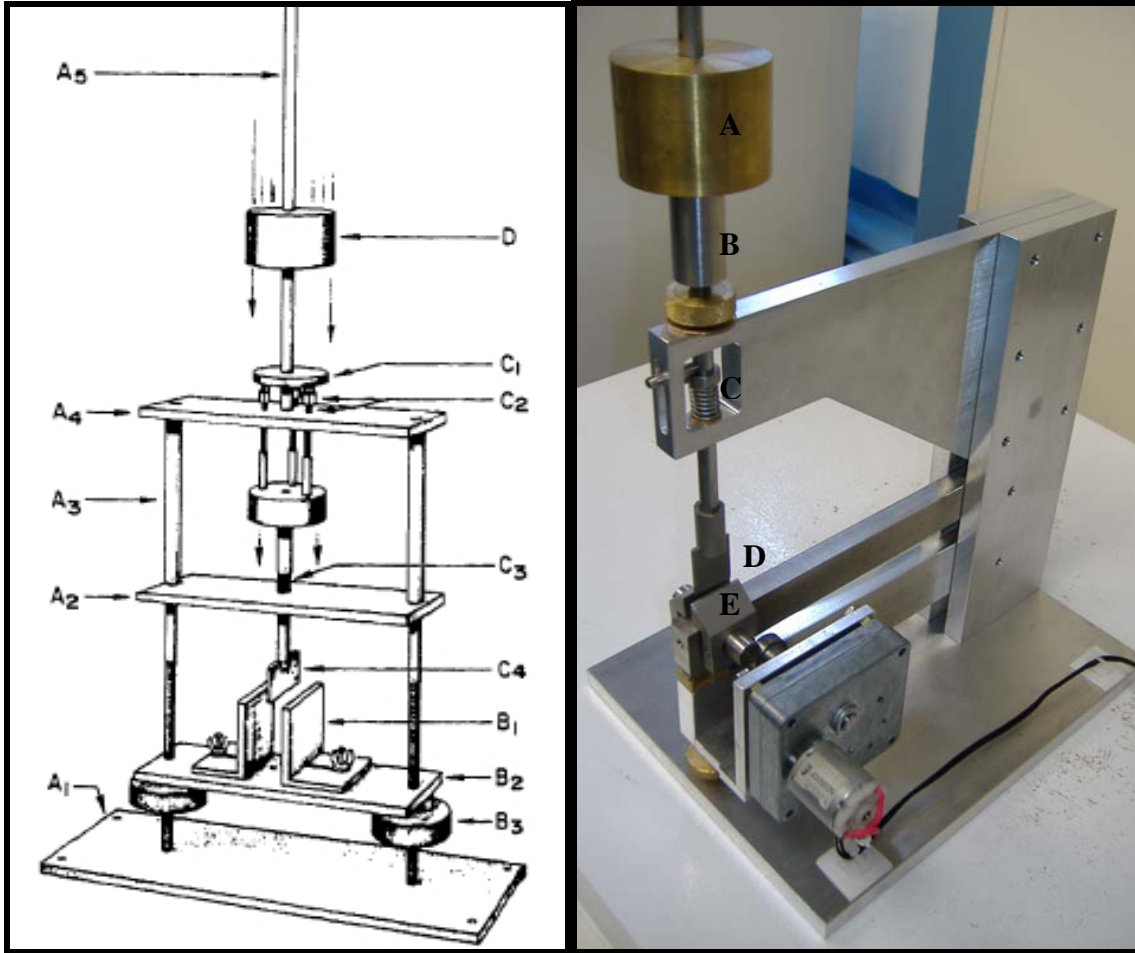
Figure 5: Illustration of Bonnarens & Einhorn's (1984) design (left, reproduced with permission from Wiley Interscience, Inc.) and Dr. Wixted's current device (right); both designs use a dropped weight to impact a shaft with the striker, use springs as a reset mechanism and require the user to properly position the mouse femur on the anvils; Legend, left: A5 – shaft, B1 – anvils, C1 – impact platform, C2 – reset springs, C4 – striker, D – impact mass; Legend, right: A – impact mass, B – impact platform, C – reset spring, D – striker, E - anvils
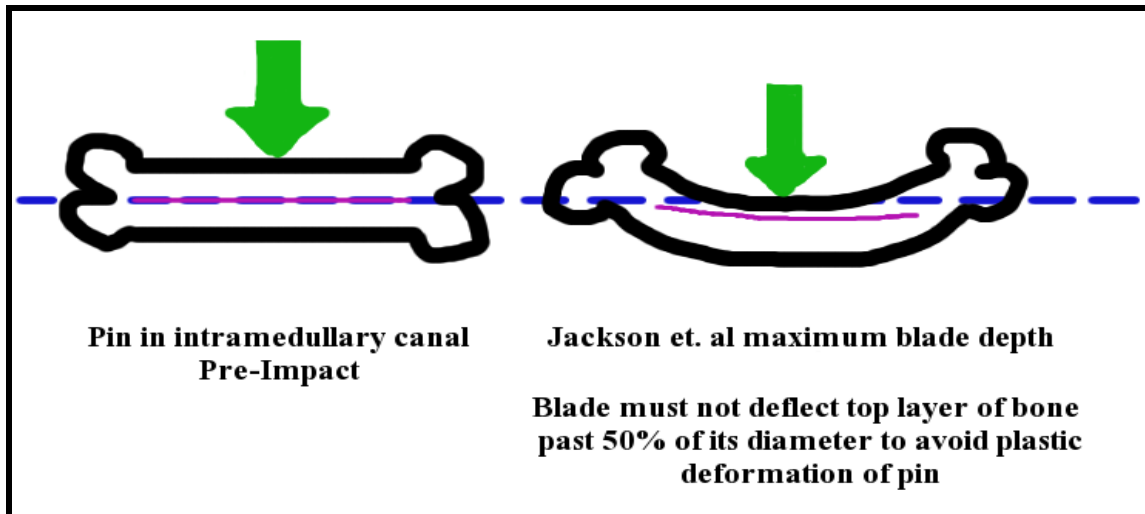
Figure 6: Illustration of the striker deflecting the top face of the femur by 50% of the bone's diameter; this is suggested limit of striker penetration by Jackson et al (1970)

The current setup that is used by a team from University of Massachusetts Memorial Hospital, led by Dr. Jack Wixted, MD, is very similar to Bonnarens and Einhorn's design (1984). This device can be seen in a side-by-side comparison with that of Bonnarens and Einhorn in Figure 5. Dr. Wixted's device uses a long shaft on which the "guillotine-style" striker is attached. This striker then rests on the femur, which is also supported by two anvils coming up from the base of the machine to achieve the three point bending. Some of the challenges with Dr. Wixted's current device are the amount of variability in how the fracture is achieved as well as the positioning of the mouse femur relative to the striker. Another difficulty is that the process requires two people - one person is needed to hold the mouse in place and another person is needed to drop the weight. Therefore a useful addition would be an attachment that can be used to position and hold the mouse in place.

Although the prior devices have been relatively successful in fracturing mouse femurs, there have been several shortcomings. One factor is that all of the devices fail to take into account the mouse leg or body. While the mouse is held in a supine position

during the procedures, the mouse body and leg are not held securely in a specific, reproducible orientation. This lack of positioning system is one of the major factors that could have led to an additional shortcoming of previous devices, which is reduced accuracy and reproducibility. The machines do not create a transverse fracture an acceptable percentage of the time; communication with experts in the field reveals that approximately 30% of fractures are not desirable (personal communication, Dr. Wixted, 2006). This is largely due to the variance in orientation of maximum force relative to the femur as well as the variability in mouse size. Durability is also a problem in designs involving springs. Over time, after a number of impacts, the stiffness coefficient of the spring decreases and the device may no longer create the desired fracture due to inconsistent impact velocity.

Another factor contributing to poor reproducibility is the number of variables in some of the devices. With many adjustable features in the user's control, achieving the desired fracture is complicated. A systemic study analyzing the different parameters contributing to a fracture and their optimization has yet to be completed. Thus the major goal of this project was to use the new fracture device and determine the ideal levels of kinetic energy to create a transverse fracture. Once established, researchers who currently use similar devices would know what impact mass and velocity they should use to obtain a transverse fracture in their mouse model. Additionally, future devices could use the data in their design and avoid costly errors from improper breaks.

3. PROJECT APPROACH

The fracture device introduced here was motivated partially by previous designs, such as the Bonnarens' three-point bending design (Bonnarens and Einhorn, 1984) and partially from an understanding of fracture mechanics. The primary issues with previous designs and the design that our client was formerly working with were unacceptable reproducibility, two-person operation and little control for modifying important parameters, such as impact velocity and mass. Our hypothesis for this project was that the independent modification of mass and velocity and the proper positioning of the mouse femur will allow for a range of break types establishing the limits of kinetic energy to create transverse fractures.

One major assumption of our experiment was that deceased mice have the same fracture properties as live sedated mice. This decision was based on a desire to use mice that were sacrificed for other experiments to avoid ethical issues. It was determined that the effect of a live mouse femur is negligible because sedation relieves any interfering muscle tension and hydrostatic blood vessel pressure is negligible compared to the stiffness and fracture toughness of the bone. Therefore, pre-sacrificed mice were used to model live mouse fractures due to the acceptance of this assumption. Another assumption was that variation of age and gender were not significant to bone properties in mice.

The specific aims of the project were based on our hypothesis and were designed to include improvements to reproducibility of fracture models and to provide useful mechanical relationships to enhance the efficacy of murine fracture experiments. These specific aims of the project are provided below:

1. Design a fracture device with precise adjustment of key parameters including impact mass, impact velocity, anvil gap and striker penetration depth.

2. Develop a novel system to remove user variance in femur positioning and ensure identical femur positioning for all experiments.

3. Create statistical model relating kinetic energy (mass and velocity), mouse mass and fracture type to further quantify murine fracture mechanics.

4. Develop a modeling equation to predict break type that researchers can easily use to find the optimal mass and velocity combinations to use on their fracture devices.

4. DESIGN

Prototyping

Before any design could be completed to find solutions to enhance fracture reproducibility, the first step was to determine what means of force generation was most appropriate. Although gravity driven designs have been prevalent in past research, they may or may not be optimal for our application. To do this, several design metrics were created to provide weight to design decisions; these are provided in Table 2.

Table 2: Design metrics based on pairwise comparison chart results

METRIC	DEFINITION	RATING
Precision	Reproducible, not necessarily desired result	5.5
Accuracy	Achieving correct break type	5.0
Reliability	Functioning without fail	4.5
Safety	Protection of user	3.0
User-Friendliness	Ease of use with all functions	2.0
Cost	Dollar value of material and associated labor	1.0
Durability	Material resistance to breakage over time	0.0

The above design metrics were based on two pairwise comparison charts, one from the design team and another from the client. They were averaged to ensure that both parties had equal influence in the initial design process. From Table 2 it is clear that the final prototype must be able to create a reproducible and transverse fracture, based on

the two highest ratings on the table. In contrast, it was agreed that cost and durability

were minor factors, due to a likely minor build cost and an assumed ease of replacement

in the event it should breakdown. These design considerations were used in determining

the weight of design objectives, including "simplicity" and "reproducible fractures".

The force-generation prototypes were designed from influences in previous

fracture designs and also from industrial machinery. A pool of over 15 possible means of

force generation for the device were reduced to four based on feasibility and likelihood of

successful incorporation into a fracture device. These means are described in Table 3.

Table 3: Force-generation prototype designs with descriptions

Means of force generation	Description	Sketch
Gravity-driven	Design uses force of gravity from adjustable mass and height to generate kinetic energy and drive striker into mouse femur. The design requires only one user by incorporating an electromagnet/foot pedal circuit for operation and reset feature. Springs are eliminated.	
Electromagnet	Design uses a pulse electromagnet to drive a magnetic piston through a vertical shaft to impact the mouse femur. The shaft would automatically reset from gravity.	
Pneumatic	Design uses a regulated compressed air source to drive a piston to impact femur. A spring inside cylinder coupled with an exhaust port enables the striker to strike and retract very quickly and automatically for efficient use.	
Cam	Design utilizes a mounted electric motor to drive a two-piece shaft to create an impact fracture. The horizontal shaft movement permits use of a full body vertical mouse board with adjustable straps.	

Each of the prototypes from Table 3 had their own unique advantages and disadvantages. To determine which means of force generation would be most suitable for the fracture device, the design metrics provided in Table 2 were used to weight the objectives of the design. Additionally, the prototypes were referenced against the constraints of the design to ensure that the final prototype would be fully compatible. Thus, the prototype that met all design constraints and fulfilled the design objectives most thoroughly was considered most appropriate. This selection matrix is shown in Table 4.

Table 4: Force-generation selection matrix with design objectives and constraints

Design Constraints		Gravity-Driven	Pneumatic	Electromagnet	Cam
Cannot cost more than $2450		Y	Y	Y	Y
Right leg only		Y	Y	Y	Y
Non-Invasive		Y	Y	Y	Y
Smaller than 3 cubic feet		Y	Y	Y	Y
Non-Comminuted		Y	Y	Y	Y

Design Objectives	Weight (%)	Score	Weighted Score	Score	Weighted Score	Score	Weighted Score	Score	Weighted Score
Closed, transverse fracture in middle 1/3 of femur	30	0.8	24	0.7	21	0.5	15	0.6	18
Reproducible fracture	25	0.6	15	0.5	12.5	0.7	17.5	0.7	17.5
Single person for operation	5	1	5	0.6	3	0.9	4.5	1	5
Simple design	15	0.95	14.25	0.5	7.5	0.4	6	0.6	9
Accommodation for different sizes of mice	5	0.7	3.5	0.8	4	0.8	4	0.6	3
Adjustable variables of kinematics	10	1	10	0.5	5	0.8	8	0.6	6
High energy impact fracture	10	1	10	1	10	1	10	1	10
TOTAL:	100		81.75		63		65		68.5

Since reproducibility and precision were ranked highly as design metrics, their related objectives were given the most weight in the ranking decisions above in Table 4. The results of this selection matrix determined that gravity would be the most appropriate

means of generating force to fracture the mouse femur. The principle issue with the

pneumatic design was that its reset mechanism required the use of a spring, whose

stiffness would decrease over time and result in less reproducibility. The electromagnet

design had several problems, including complexity and difficulty in targeting due to the

striker orientation. Similarly, the cam design was complex from its non-cyclic nature and

had positioning issues for the mouse femur. In contrast, the gravity design was a simple,

fully adjustable and reproducible means of force generation.

A prototype selection matrix (SM) was subsequently applied to three gravity-based

designs in a similar method as above to determine the most appropriate means of utilizing

gravitational force for the fracture device (SM provided in Appendix A1):

- *Uniaxial* – Design uses force of gravity from adjustable mass and height to generate kinetic energy and drive striker into mouse femur. The design requires only one user by incorporating an electromagnet/foot pedal circuit for operation and reset feature. Springs from traditional designs are eliminated. (SM score: **87**)
- *Pendulum* – Design uses a triangular support to propel a striker through a one-dimensional 360° rotation (no movement in r or z directions). Mouse is positioned for impact immediately underneath supports for horizontal impact, as per Charpy impact test specifications. User would be able to modify height in order to change kinetic energy. (SM score: **77.5**)
- *Incline Plane* – Design incorporates a low friction surface and rails to guide a striker-on-wheels to impact mouse leg. A stop at the bottom position determines depth of striker penetration. Mouse position is perpendicular to incline surface. User would be able to adjust weight of striker cart and distance of striker descent. (SM score: **61**)

The results of the selection matrix showed that the uniaxial design was the

superior design by a significant margin. Although pendulum designs are commonly used

for fracture testing, the nature of the pendulum required a vertical orientation of the

mouse, which would result in less reproducibility from difficult positioning of the femur.

The principle issue with the incline plane was also reproducibility, from the high friction

on the plane that would slow the cart differently each test. It was easier to simply drop

the weight from a 90º angle as in the uniaxial design, than to design a low friction incline plane. Thus, the outcome of brainstorming, pairwise comparison charts and selection matrixes was that the most appropriate design for this application was a uniaxial, gravity-driven fracture device.

Design parameters and specifics

With a uniaxial gravity-driven design in mind, the next step in the design process was determining how the device would accommodate different size mice. The study of fracture mechanics provided in the Background section showed that modification of kinetic energy at impact would provide a means of adjusting for different sized mice which may have stronger or weaker femurs. Along with *mass* and *velocity* from the kinetic energy equation, the distance between the anvils for three-point bending ("*gap*") and the *depth* that the striker deflected the femur would modify the kinetic energy necessary to fracture it. A schematic representation of these four variables is provided below in Figure 7.
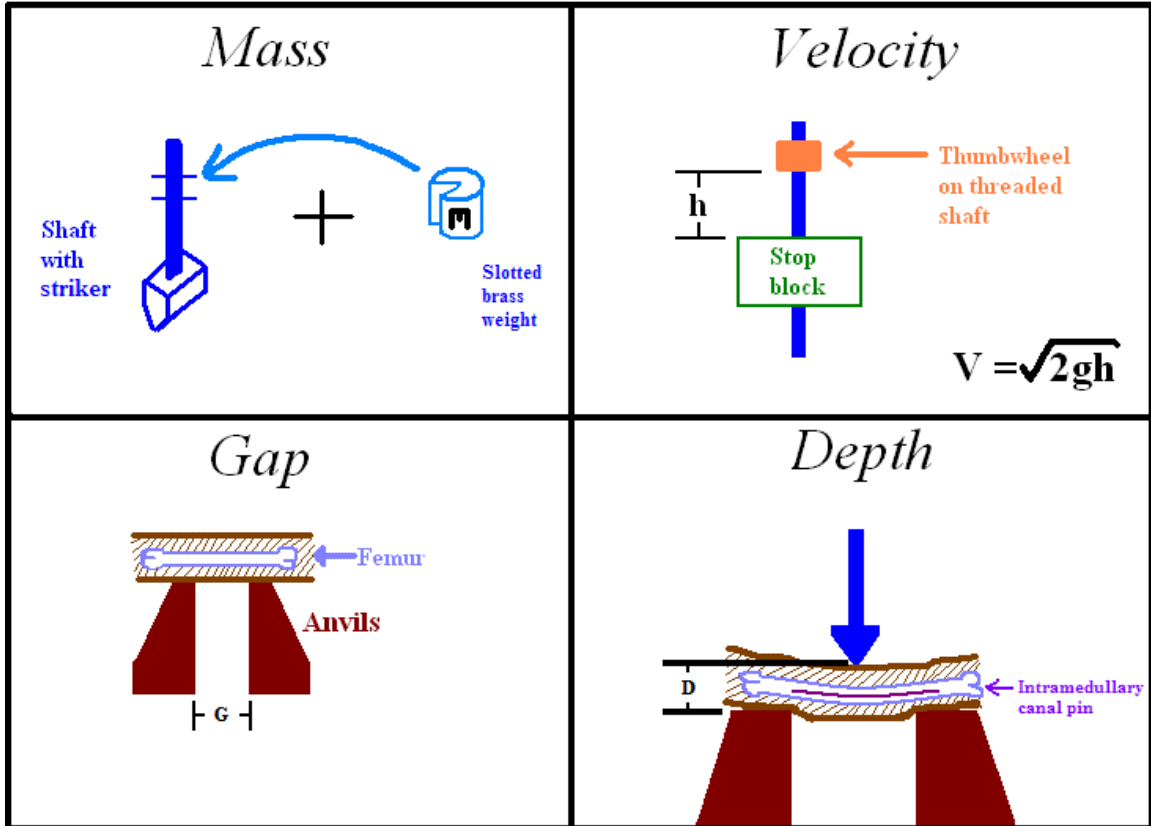
Figure 7: Four variable parameters in the prototype fracture device; (Top) adjustable mass and velocity change kinetic energy (Bottom) gap distance and striker depth modify level of kinetic energy necessary to fracture femur

For user simplicity, it was decided that the device should have a partially-fixed anvil gap distance and a partially-fixed striker depth. This would enable the user to adjust the variables if desired, but for the majority of operation (such as the same species of mouse but different mouse masses) they would be kept constant. The determination of appropriate gap and depth is provided in the Methods section, along with an outline of testing procedures for mass and velocity optimization for different sized mice.

Traditional designs such as the Bonnarens and Einhorn (1984) device use a shaft with an end-striker (see Figure 5 for schematic) positioned directly above the femur. The shaft is then impacted by a dropped weight that causes the striker to drive into the femur. For the design proposed in this paper, rather than having the shaft and impact weight be

two separate parts, the impact weight was eliminated and the shaft itself was the weight (see Figure 9). The mass of the shaft can be adjusted by adding small brass fitted weights fixed to a threaded portion of the shaft by nuts and washers. The velocity of the striker at impact can be adjusted by changing the vertical position of a thumbwheel on a threaded portion of the shaft, instead of changing the height that the separate weight was dropped from (see Figures 5 and 12). The different positions would allow different times in freefall and thus different velocities at impact. The velocity positions required the anvils that hold the femur to vertically adjust as well, which meant that the base stage needed to correspond to the thumbwheel height changes. Without this adjustability of the base, the striker would penetrate through the bone or may not even touch the animal (see Figure 13). Rather than having a continuously adjustable base, five different velocity positions were created to maintain a high level of controlled variability while still providing a solid base for impacts. Note that the shaft was considered to be in a frictionless free-fall through the linear bearings, which enabled measurement of impact velocity from basic physics ($V = \sqrt{2gh}$, see Figure 7).

With the four parameters designed for, the next major challenge was to design a reset mechanism that could drop and pick up the adjustable-mass shaft. As stated in the Background section, the two principal issues with previous fracture devices have been the use of springs to provide force to retract the shaft and a requirement for two-person operation (one to position the mouse and another to drop the weight to impact the shaft). The design proposed here omitted springs to ensure constant reproducibility and instead uses a magnet and electromagnet assembly (see Figure 10). The shaft can be fixated with powerful neodymium magnets that are attracted to an electromagnet.

In the powered-on and closed circuit position, the shaft is held well above the femur at the desired height based on impact velocity. On command from the user, the depression of a foot pedal opens the circuit and cuts the magnetic attraction from the shaft and magnets, causing the striker to fall. When the foot pedal is released, the electromagnet is engaged and could theoretically pull the striker up to the starting position. If the pull of the electromagnet on the shaft and magnets is too weak to lift them up from the lowest position, the shaft could be manually lifted until the magnetic attraction holds the striker assembly in place. In the ideal operation, one person can easily use the device, even without using their hands. The shaft is also able to reset without the use of springs. Possible friction concerns are minimized through the use of a dual linear bearing setup. These linear bearings promote near-frictionless linear motion along the axis of the shafts, while preventing rotational movement of the striker assembly, thus keeping the striker head parallel to the anvils.

The final design area was concerned with positioning of the mouse itself. The study of fracture mechanics provided in the "fracture theory" section of the Background noted that three-dimensional orientation of the femur relative to the striker was critically important for the end fracture result. If the orientation was offset from perpendicular by a significant degree, than an oblique fracture could result. Thus the method to stabilize and position the mouse body and femur were essential to the function of the fracture device.

The novel mouse positioning system (MPS) proposed in this paper is composed of three principal components, based off of the area of the mouse they stabilized. First, the torso is stabilized by a half-pipe, which was chosen out of four potential candidates by a selection matrix (provided in Appendix, Table A2). These candidates included a flat

table, a table with a mold, an inclined plane and a half-pipe. Ultimately, the half-pipe

provides the easiest and simplest access to the mouse while still providing multi-planed

support. Additionally, the half-pipe permits easy maneuverability of the torso through

rotational and vertical displacement. To stabilize the tibia, a single 316 stainless steel

clip was implemented on the distal anvil to create a 55° angle between the femur and

tibia. An angle greater than 45° was desired to minimize interference of the

intramedullary canal pin (important for intramedullary canal positioning in the Methods

section) used for fracture fixation. Finally, the femur itself was stabilized by a dual 316

stainless steel clip system that was anchored in the side of each anvil and protruded over

them. These design sketches are provided in Figure 8:
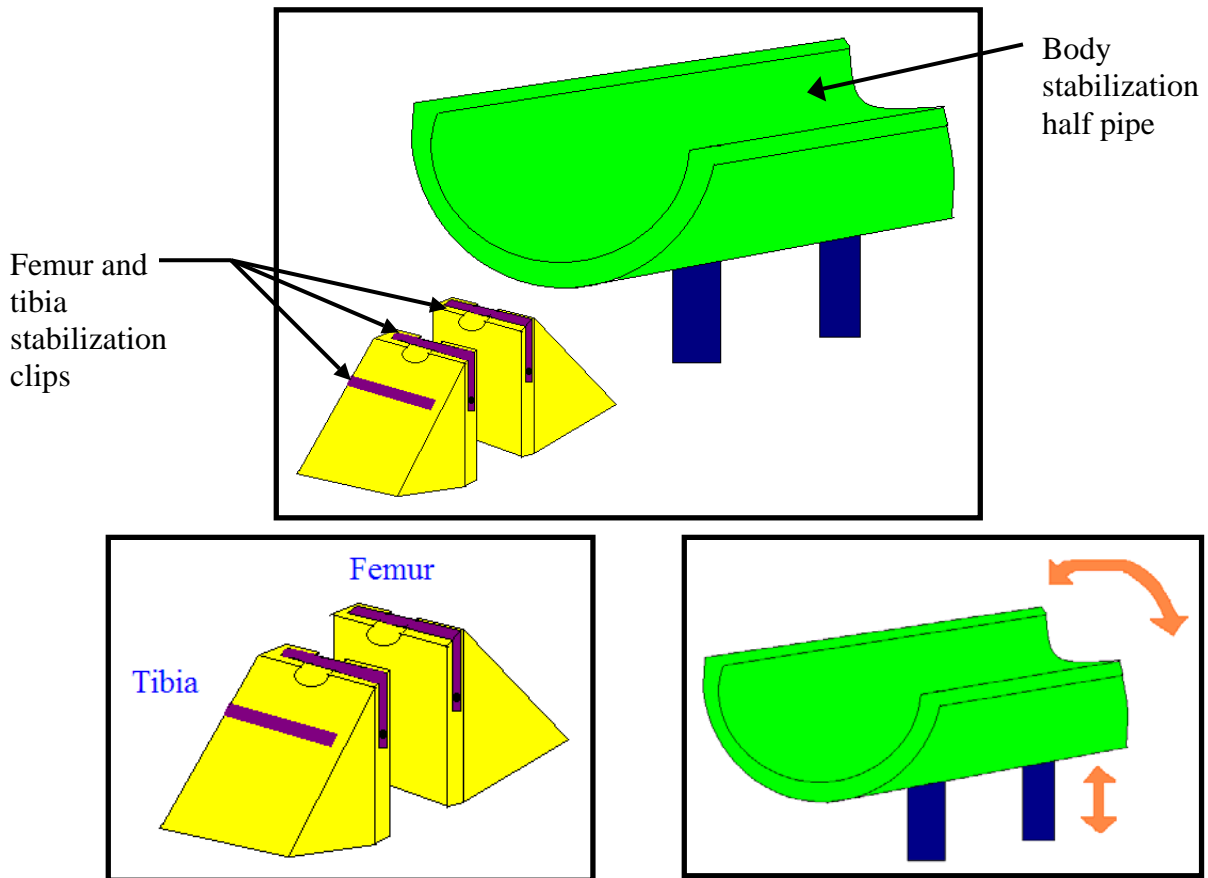
Figure 8: Schematic of Mouse Positioning System (MPS) components; triangular anvils are equipped with three stainless steel clips to stabilize femur and tibia, and half-pipe provides bodily support while permitting rotation of torso to allow left or right femur accessibility

In summary, initial design considerations from research and our client statement led to selection of a final prototype. The shortcomings of previous femur fracture designs are overcome through the implementation of a novel femur positioning system and the use of kinetic energy as the primary fracture parameter.

Design drawings

Before constructing the prototype based on the above design approach, the design was drawn in a 3D modeling program (Pro/Engineer, PTC, Needham, MA) to ensure that it would be assembled and manufactured properly. All dimensions were carefully determined and parts from vendors were incorporated in real scale. Figures 9 through 16 below provide an overview of the entire assembly and its components:
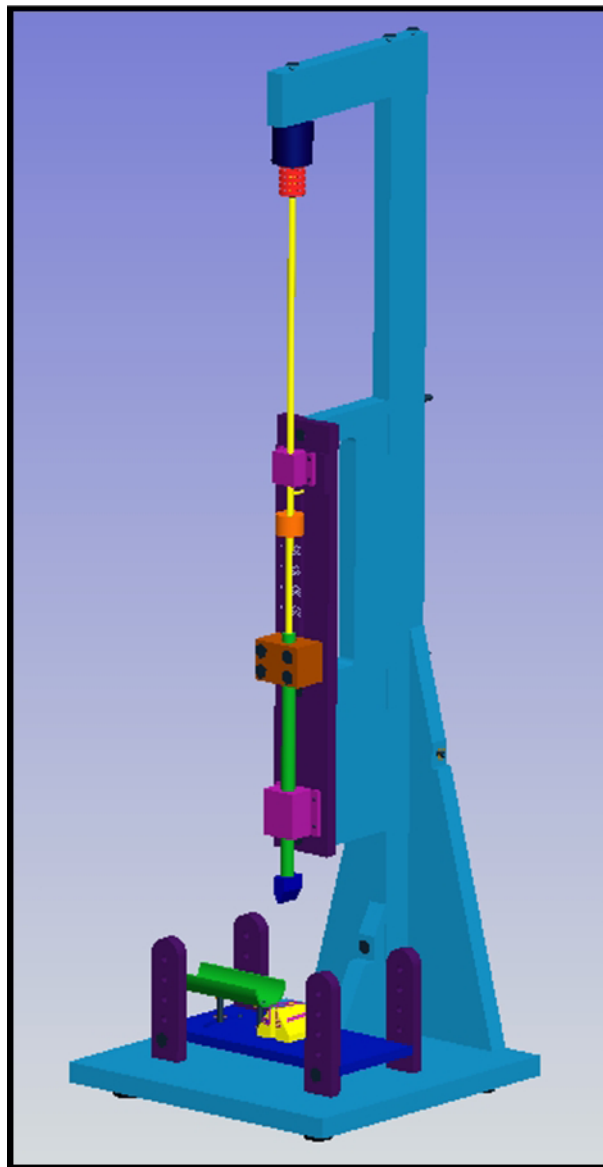
Figure 9: Assembly overview of prototype uniaxial gravity-driven fracture device
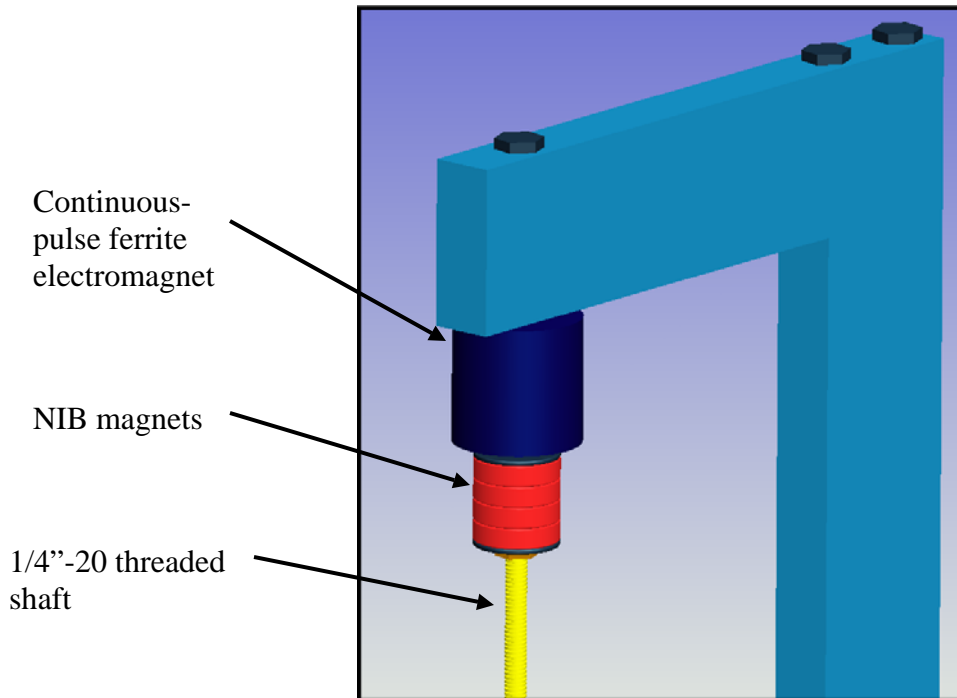
Figure 10: Electromagnet release system with Neodymium-Iron-Born (NIB) magnets and threaded shaft area to add mass

Continuous-pulse ferrite electromagnet

NIB magnets

1/4"-20 threaded shaft
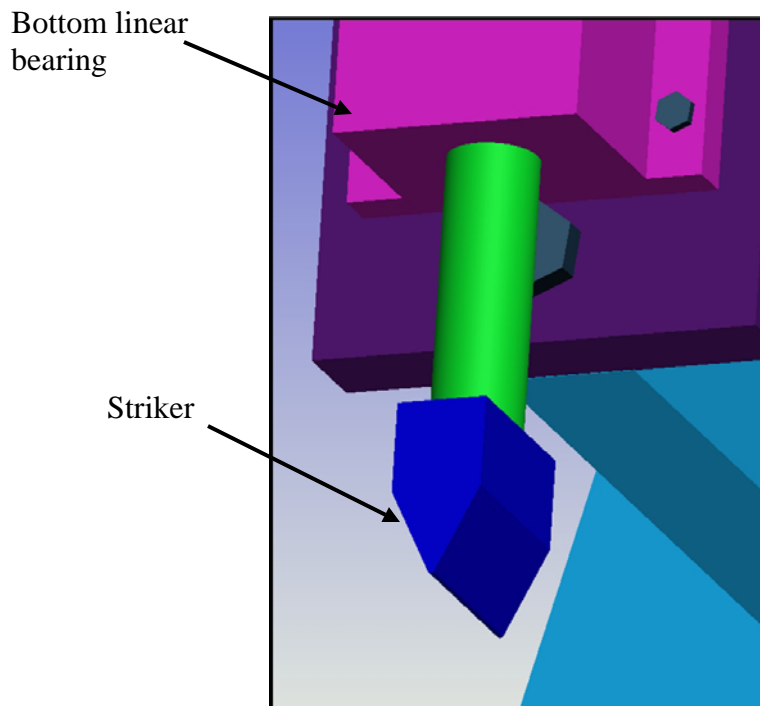
Figure 11: Fracture striker with rounded, blunt tip

Bottom linear bearing

Striker
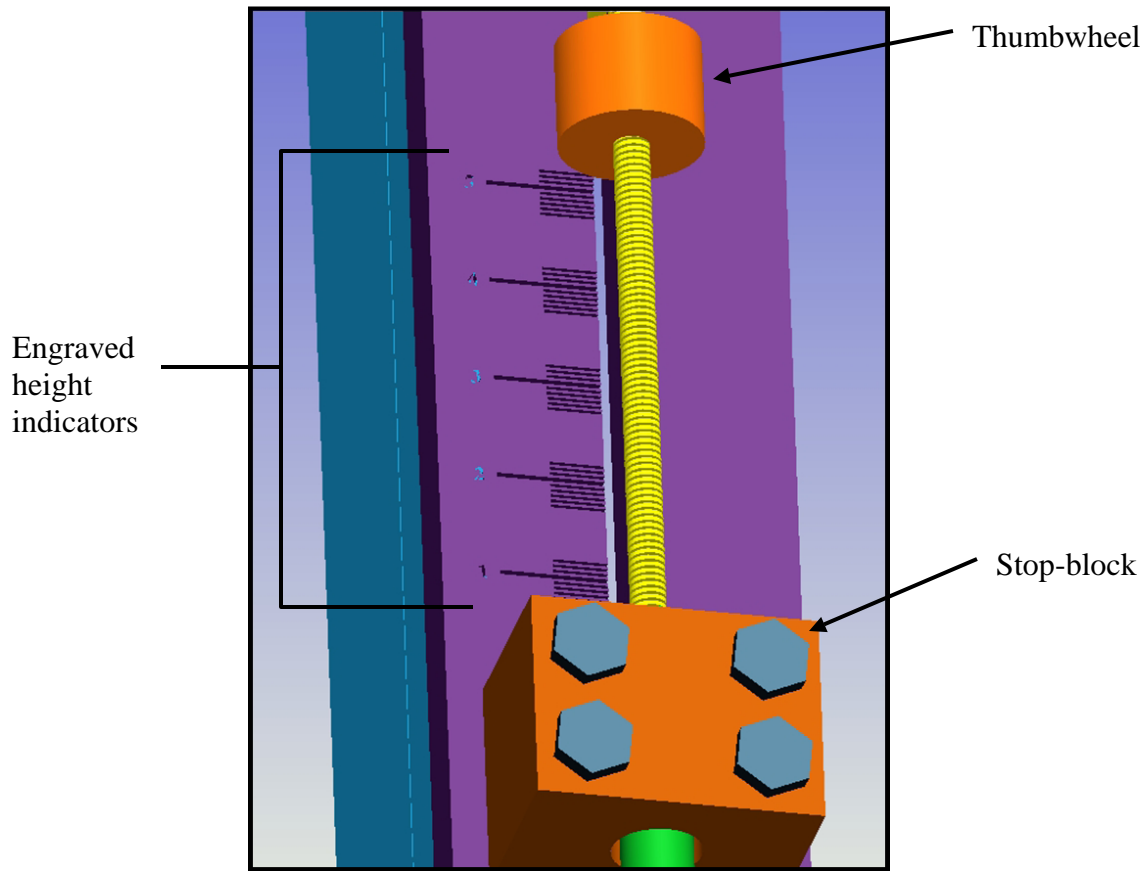
Figure 12: Thumbwheel impacts stop-block; incremental height indicator for height reference (see Figure A1 in Appendix for detail drawing of plate)
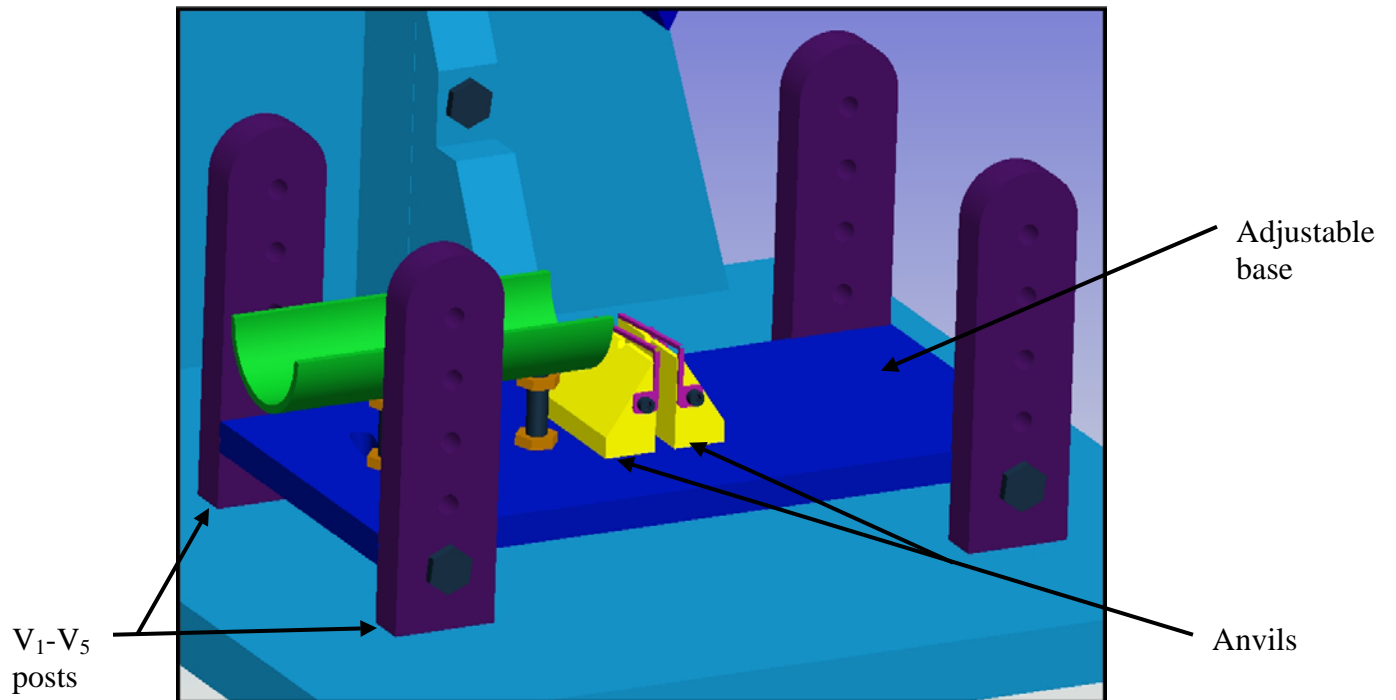
Figure 13: MPS adjustable base, variable velocity posts & three-point bending anvils (see Figure A2 in Appendix for detail drawing of adjustable base plate)
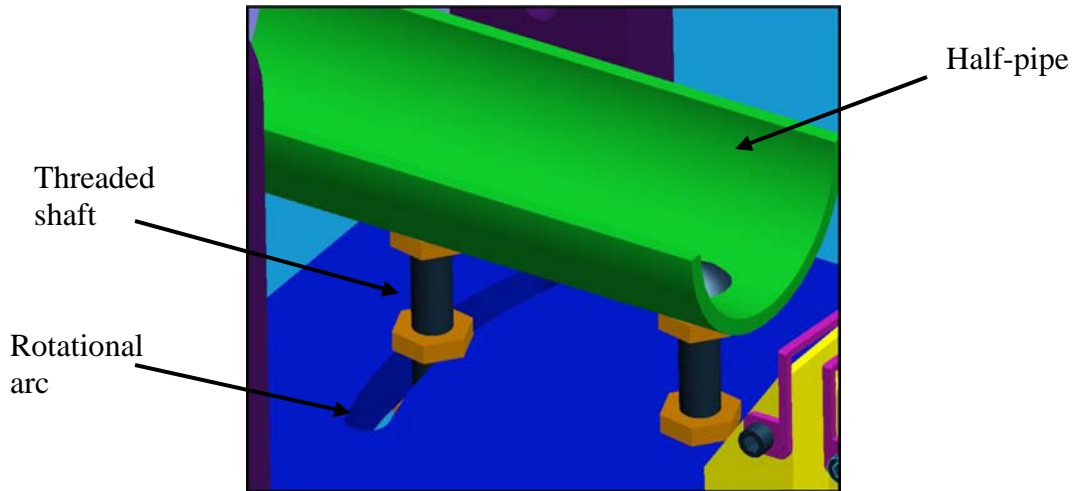
Figure 14: MPS half-pipe with rotational arc and threaded shaft for vertical movement
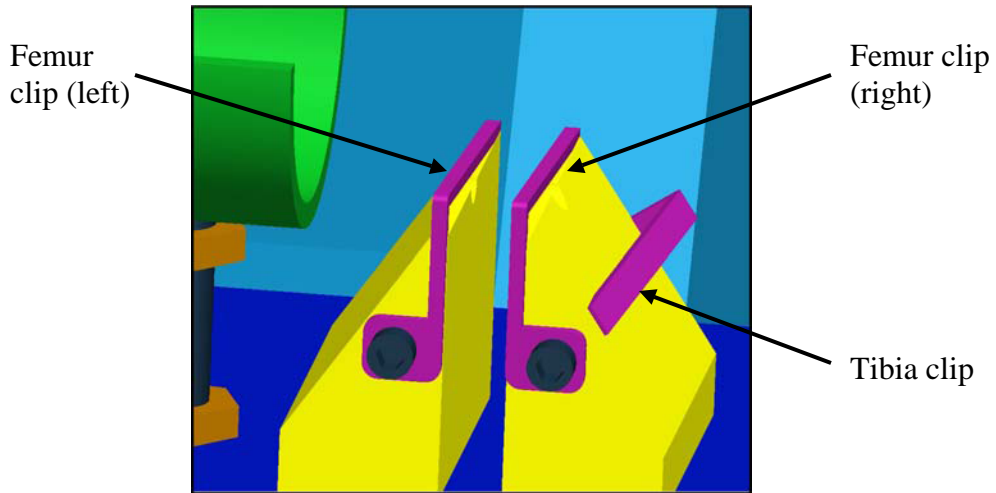
Figure 15: Two MPS femur clips and MPS tibia clip
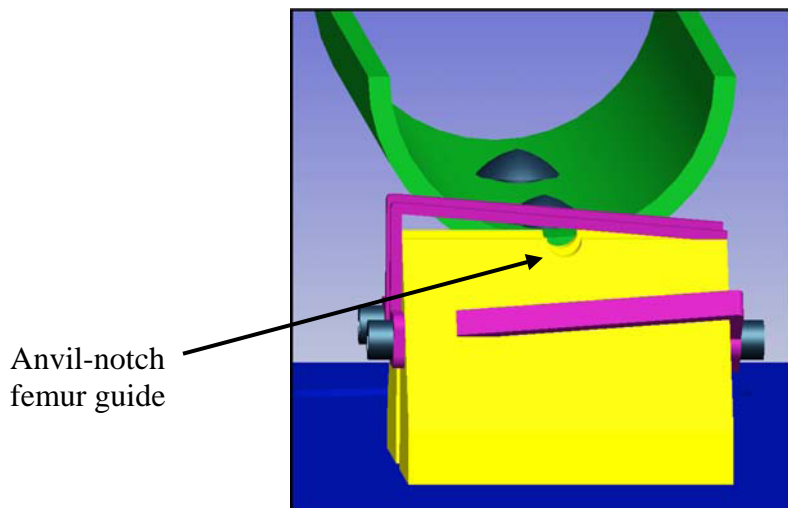
Figure 16: Femur alignment into anvil guide indentations from half-pipe (see Figure A3 in Appendix for detail drawing of anvil)

Materials

The materials of the above design were chosen based on the design criteria in

Table 2 with additional consideration from their load bearing properties, ability to be

cleaned, corrosive properties and weight. The materials used for the prototype were:

- 316 stainless steel – used in materials that contacted the mouse to permit the use

  of strong chemical cleansers without corrosion and parts requiring high flexural

  strength; these included the halfpipe, anvils, femur and tibia clips, fracture striker

  and three major load bearing bolts

- 440 C stainless steel – used in precision lower shaft (Figure 11, green) for its

  excellent machinability for a tight diameter match (class 6g tolerance) in the

  lower linear bearing to minimize friction

- Brass – used in slotted weights to add additional mass to the shaft

- Neodymium – grade N45 neodymium-iron-boron magnets used for release

  mechanism

- Aluminum – used for all other parts for its machinability, specific strength and

  corrosion resistance

Final design assembly

After machining all parts to specifications in the computer model, the parts were

assembled using mostly bolts and threaded rods. The specific bolts and fasteners used,

along with all parts and total cost, are provided in a full parts list in the Appendix under

Table A5. The electromagnet wiring was braided to reduce clutter and a master control

box was designed to eliminate the need of the user to unplug the power supply to

disengage the circuit. A final incorporation of an orange LED was added to the control

box to provide confirmation to the user that the circuit is closed and operational. After

assembly was completed, the next step was testing and validation, which is subsequently

described in the Methods section. An isometric photograph of the assembled final design

is provided in Figure 17 and a detail photograph of the MPS is provided in Figure 18.
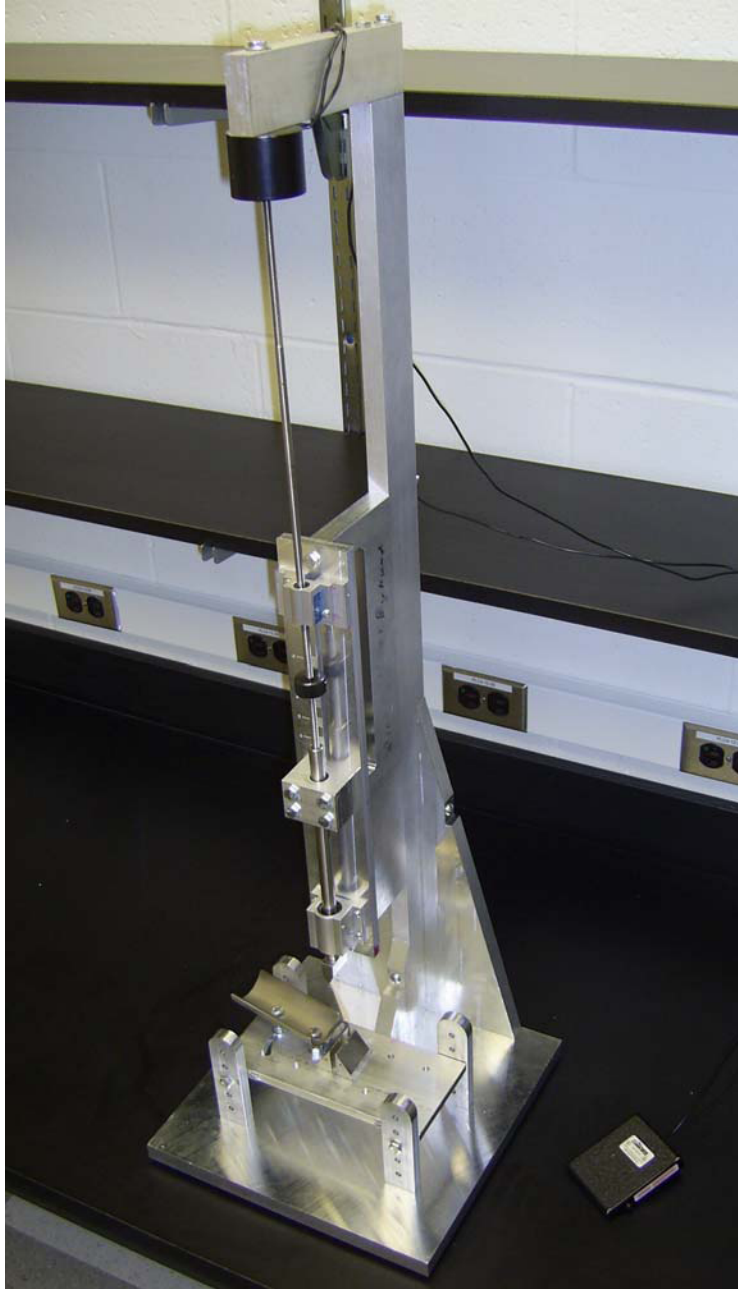
Figure 17: Isometric photograph of constructed prototype
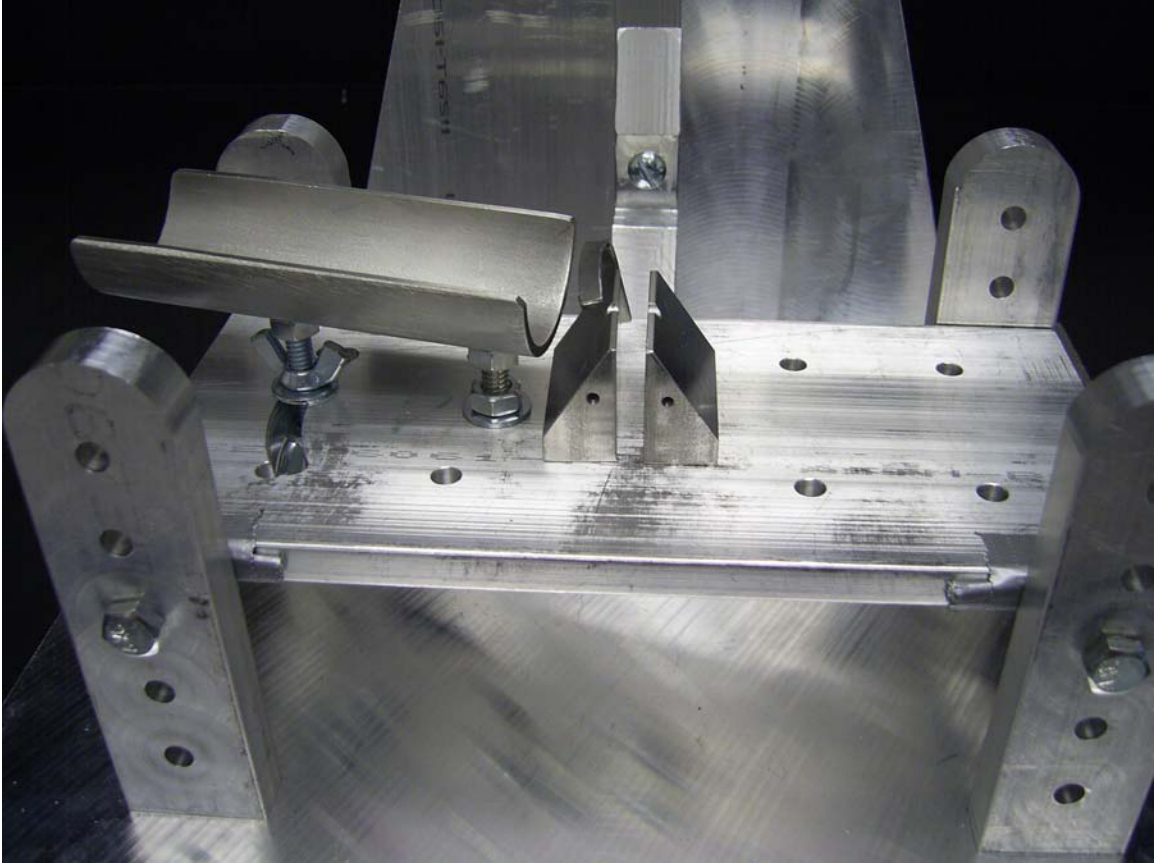
Figure 18: Detailed photograph of mouse positioning system as built in prototype

5. METHODS

In order to validate that our device was capable of adjusting kinetic energy parameters, it was first necessary to experiment with a number of mice to find the range of break types possible with a set geometry. There are four variables that can be adjusted and controlled on the device: the local depth of the striker relative to the anvil height (D), the horizontal gap distance between the anvils (G), the velocity of the striker at impact (V), and the mass of the striker and shaft system (M). See Figure 7 in the Background section for the schematic representation of these four modifiable variables.

The only other factor to consider was the weight of the mouse (W) in the fracture experiment. A larger mouse was theorized to have a thicker and stronger femur, so a higher kinetic energy would be required to fracture it properly. The following tests involved the factor W in order to identify the kinetic energy needed to break mouse femurs of different sizes. The specific mouse groups are provided in Figure 19, which were designated to produce equal populations of mice per group. The mice were used post-mortem from other experiments ongoing in the UMass Memorial Hospital animal research lab to avoid having to sacrifice mice ourselves and possible ethical issues.
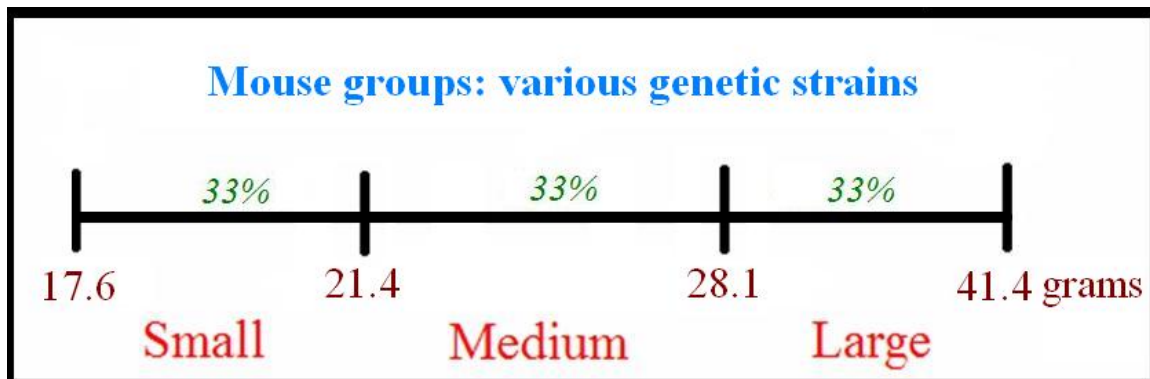
Figure 19: Three experimental mouse groups chosen from the one-third and two-third medians of the mouse weight populations

Before each of the tests were performed, a 30-gauge (0.254 mm diameter) intramedullary pin was surgically inserted into the femoral canal (as seen in purple in Figure 7). This was performed in a sterile environment and in the same manner each time. The pin was to prevent the striker from penetrating through the cross section of the femur and also aids in the healing process of the live mice, for the later part of this overall study.

There were three qualitative results for data collection. The type of break achieved was the data collected, and the four types possible were no break (N), transverse break (T), oblique break (O), and a comminuted break (C). In finding the distribution of Ns, Ts, Os and Cs, it was possible to find the best values for each variable, to produce the desired transverse break more often. It was hypothesized that in each test, the data in Figure 20 would be produced. For each test, if both variables are to one extreme, there would be no fracture, and if they are to the other extreme, they would produce a comminuted fracture. It is some central combination of the two that will produce the desired transverse fracture.
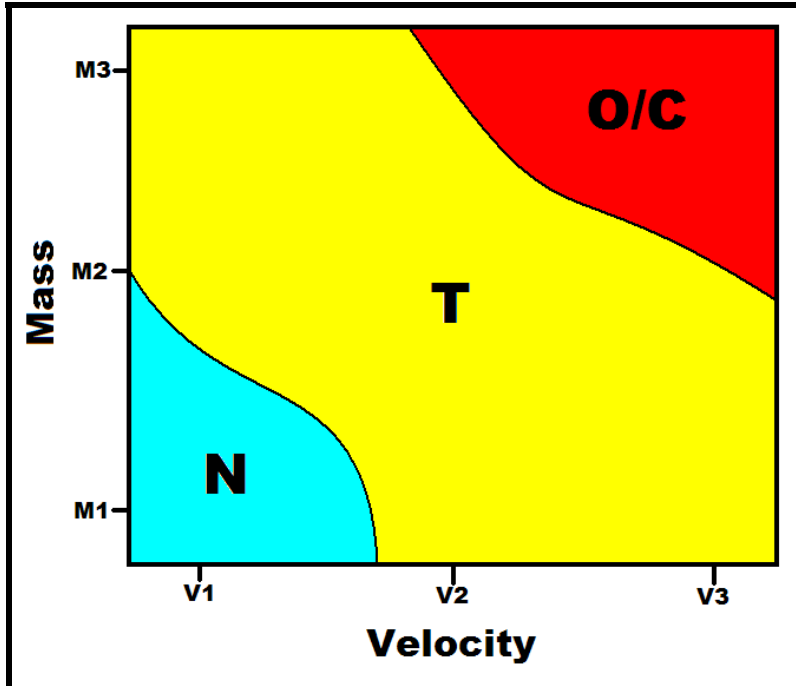
Figure 20: Theoretical fracture type results for comprehensive testing with mass and velocity; ideal combination of mass and velocity lies in the center of the T (transverse) zone for each weight group

Variables D and G were the first to be optimized, through a simple test involving six (6) mice. A fracture test was performed on both femurs of each mouse, for a total of twelve tests. Figure 7 illustrates the dimensions involved in the setup of this experiment, with the additional variable D_0 as defined in Figure 21. This would be experimentally measured by the vertical location of the intramedullary canal pin as it protrudes out of the femur. Table 5 outlines the tests performed.
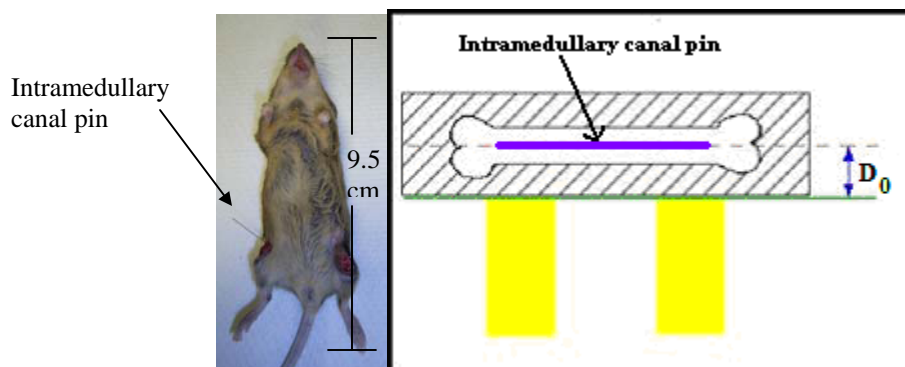
Figure 21: Variable D_0 as a reference depth value from intramedullary canal pin location; this is suggested maximum depth of striker from Jackson et al (1970)

Preliminary test protocol

Table 5: Preliminary test plan with variable depth and six mice

D=2mm	D_0	$D_0 + 0.50$mm
M_{1L}	M_{3L}	M_{5L}
M_{1R}	M_{3R}	M_{5R}
M_{2L}	M_{4L}	M_{6L}
M_{2R}	M_{4R}	M_{6R}

The mice used for this initial testing all fell into the smallest weight class, with a mass of approximately W=20g. A minimal velocity and mass was used to ensure compatibility. This was done because if the depth did not break the bone of the smallest mouse, it would not break a larger one either. Based on the client's current fracture device, G was set to 6mm for initial testing, and it was hypothesized that this would remain at this gap distance. If the results had shown that a different G was necessary, it could be adjusted first in 1mm increments either way, and then in smaller increments if necessary afterward. The depth D was set to 2mm first for four breaks, then to D_0, and finally to D_0+0.50mm. By performing four drops at each depth, the most appropriate D could be identified. This would correspond to a correct kinetic energy level requirement.

After D and G were optimized, the variables of kinetic energy, V and M, were subject to similar analysis. This experimental protocol is outlined in Table 6.

Comprehensive test protocol

Table 6: Comprehensive test plan with impact mass and velocity as variables for three separate mouse groups (testing was replicated three times for different weight mice); experimental output was fracture type as no break (N), transverse fracture (T) or comminuted/oblique fracture (O/C), pin deformation was also recorded; 1, 2 and 3 refer to small, medium and large mouse weight groups

	$M_1=350g$		$M_2=440^1$, 450^2, 460^3g		$M_3=530^1$, 550^2, 570^3g		$M_4=620^1$, 650^2, 680^3g	
V_1 (0.98 m/s)	[N, T, O/C], θ							
V_2 (1.16 m/s)								
V_3 (1.31 m/s)								

This protocol in Table 6 was followed for the three mouse groups in Figure 19 separately. The mass increments in the first row were scaled for two reasons: first, to have an equal impact mass per mouse weight, *"M/W"* ratio increase and to provide more data points for a statistical analysis. The first mass, M_1 composed of the upper and lower shaft, the slotted brass weight nuts and the striker. It was found that the magnets were not necessary to hold the shaft in place, even with a total weight of 680g, and therefore were not included in the testing.

The leftmost column of Table 6 displays the three tested velocities, one at the top level of the MPS bed (lowest velocity or V_1), one at lower level (V_2), and one at the middle level (V_3). So at each W and V there is a quadrant, representing four (4) femur fracture drops with a corresponding square. In each test square (the smallest squares on the table), there were two observations made: the type of break (N, T, O, or C) and whether or not the pin was deformed (Θ).

This comprehensive test was designed to include 4 mass levels, 3 velocity levels, 3 mouse weights, and 4 fractures per combination, for a total of 144 fracture trials on 72 mice. However, rather than testing every possible break, some assumptions were made based on patterns. Specifically, if the lowest mass (M_1) caused consistent comminuted/oblique fractures at a velocity level (V_3), then any higher masses at V_3 were assumed to also be comminuted and were excluded from testing. As the testing proceeded, such assumptions were made and the total number of fracture trials was 120, on a total of 61 mice. Fractures were performed on both femurs to use the mice to their fullest potential; however some protocols, including our client's, only specify the use of the right femur.

The data from this experiment were analyzed using a statistical significance analysis, in SAS software. The program created multi-predictor regression models for break type, using inputs of *W, M, V*, and numerical combinations of those inputs. For each model, SAS calculated the statistical significance of model equation as a prediction of break types, as well as the significance of each predictor in the equation. The best model was chosen by first considering only models with significant equations, then from those picking the model(s) that did not have any insignificant predictors.

The preliminary test combined with the comprehensive test would either confirm or refute our hypothesis, which was that optimizing mass and velocity and the proper positioning of the mouse femur will describe the best range of these variables in achieving a reproducible transverse fracture.

6. RESULTS

Preliminary test results

The experimental protocol was divided into two parts, and so the results will also

be presented in two parts. After testing the basic function with thin strips of balsa wood

to ensure consistent operation, the first half of the experiment was the preliminary test

with twelve deceased low weight mice. The objectives of this test were to see if the gap

distance or depth of striker penetration needed to be changed before the comprehensive

test. This test used the 30-gauge (0.254 mm diameter) stainless steel intramedullary

canal pins to simulate as close as possible what the comprehensive test would be like.

The results of the first preliminary test are provided in Table 7.

Table 7: Preliminary test results demonstrating ability of machine to create transverse and other fractures with gap distance of 6mm and depth of 2mm; (N) No fracture, (T) Transverse fracture, (O) Oblique fracture, (C) Transverse fracture

No. and mouse leg	Mouse weight (W)	D	Kinetic Energy – Velocity and Mass at impact (E_K)	Break type (N,T,C/O)
1 – left	18.61	D_0	V_1, M_0	N
1 – right	18.61	D_0	V_1, M_0	N
2 – left	19.06	D_0	V_3, M_0	N
2 – right	19.06	D_0	V_3, M_0	N
3 – left	21.15	D_0	V_2, M_0	N
3 – right	21.15	D_0	V_2, M_0	N
4 – left	22.65	2 mm	V_1, M_0	T
4 – right	22.65	2 mm	V_1, M_0	T
5 – left	23.77	2 mm	V_1, M_0	T
5 – right	23.77	2 mm	V_1, M_0	C
6 – left	26.58	2 mm	V_2, M_0	C
6 – right	26.58	2 mm	V_2, M_0	T
7 – left	33.96	2 mm	V_3, M_0	O
7 – right	33.96	2 mm	V_3, M_0	O
8 – left	35.19	2 mm	V_4, M_0	O
8 – right	35.19	2 mm	V_4, M_0	T
9 – left	38.47	2 mm	V_4, M_0	C
9 – right	38.47	2 mm	V_4, M_0	T

Comprehensive test results

The comprehensive test composed of 61 wildtype mice of various strains with an average mass (W) of 26.4±6.1g and a range of 17.0 - 41.4g. The total number of fractures was 120, due to complications with one leg of two mice. As in the preliminary results, a 30-gauge stainless steel needle acted as an intramedullary canal pin and the gap distance between anvils was set to 6 mm. Since no breaks were achieved using a depth of D_0 and a range of fractures were achieved using $D = 2$mm, the depth was set to 2 mm for the experiment. After each fracture, radiography was used to determine break type, which were individually and blindly verified by an orthopaedic surgeon at UMass Memorial Hospital. Examples of transverse, comminuted and oblique fractures are provided in Figure 22 and the results of each experimental fracture are provided in Table 8. Additionally, graphical representations of Table 8 are provided in Figures 23 and 24, which are a population density histogram and a contour plot of fracture results, respectively. The first graph shows how the mouse weights were distributed, and the second shows fracture results of all mice without reference to mouse weight.
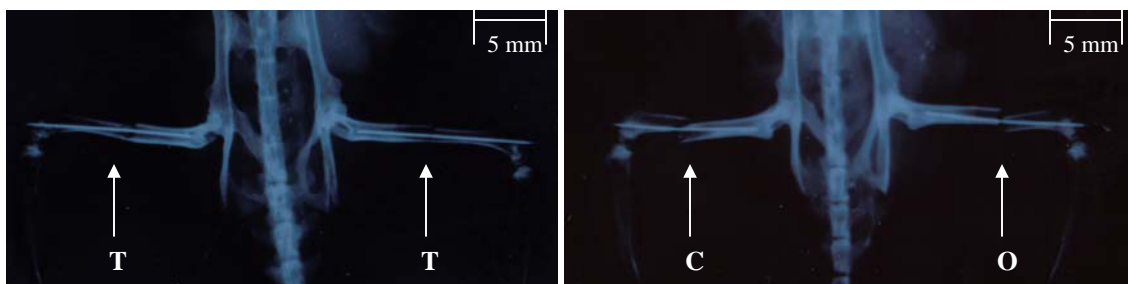
Figure 22: Radiograph examples of transverse fractures (left, ID#45) and comminuted/oblique fractures (right, ID#50); fracture type determined by orthopaedic surgeon J.Wixted, MD, University of Massachusetts Memorial Hospital

Table 8: Test results using mice weighing between 17-41g and using various kinetic energies; (N) No fracture, (T) Transverse fracture, ideal, and (O) Oblique fracture and (C) Comminuted fracture

Mouse weight (*W*), grams	Mouse ID #	Group #	Impact mass (*M*), grams	Impact velocity (*V*), m/s	Break Type - Left	Break Type - Right
17.6	5	1	350	0.98	N	O
18.8	1	1	350	0.98	N	T
18.9	43	1	440	0.98	C	T
19.1	53	1	540	0.98	T	
19.2	2	1	350	0.98	N	N
19.5	45	1	440	0.98	T	T
19.8	16	1	450	1.16	T	T
19.8	54	1	540	0.98	T	T
19.9	12	1	550	0.98	T	T
20.4	37	1	440	0.98	T	O
20.5	4	1	350	0.98	N	C
20.5	13	1	350	1.16	T	N
20.8	15	1	450	1.16	T	O
20.9	3	1	450	0.98	T	N
21	11	1	550	0.98	T	T
21	14	1	350	1.16	O	O
21	17	1	350	1.31	C	O
21.1	36	1	350	0.98	T	T
21.4	9	1	450	0.98	C	T
21.4	55	1	350	1.16	T	T
21.5	38	2	350	0.98	T	T
22.2	39	2	570	1.31	O	T
22.2	46	2	460	1.16	T	T
22.2	56	2	350	1.16	C	O
22.6	47	2	460	1.16	O	O
23.7	52	2	580	1.31	T	T
23.8	35	2	570	1.31	T	T
24.2	44	2	350	0.98	T	T
25.2	6	2	350	0.98	T	T
25.2	21	2	350	1.16	T	O
26	8	2	460	0.98		T
26.5	10	2	460	0.98	T	T
26.6	60	2	680	1.31	T	C
26.8	7	2	350	0.98	T	T
26.8	23	2	460	1.16	T	T
26.8	25	2	570	1.16	O	O
27	18	2	570	0.98	C	T
27.1	24	2	460	1.16	T	O
27.5	19	2	680	0.98	T	T
28.1	26	2	570	1.16	T	T
28.3	22	3	350	1.16	T	T
28.6	27	3	350	1.16	O	C
29.1	20	3	680	0.98	T	T
29.2	61	3	570	1.31	O	O

29.9	59	3	680	1.16	C	T
30	58	3	680	1.16	T	O
30.5	51	3	460	1.31	T	T
30.7	30	3	680	1.16	O	O
31.9	42	3	450	0.98	T	C
32.6	57	3	460	1.16	O	T
33.6	49	3	350	1.31	T	T
34.4	28	3	350	1.31	O	T
35	29	3	680	1.16	O	T
35.1	40	3	570	1.31	O	O
35.2	50	3	460	1.31	C	O
36.3	32	3	350	1.31	T	O
36.4	33	3	460	1.31	O	O
36.8	41	3	680	1.31	O	O
38.8	31	3	680	1.31	O	O
39.8	48	3	350	1.31	T	T
41.4	34	3	460	1.31	O	O
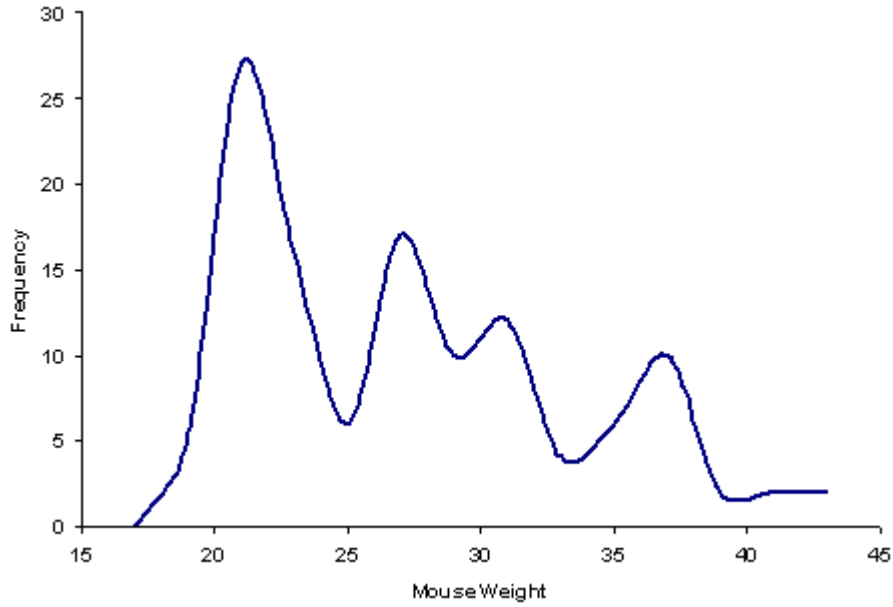
Figure 23: Population density histogram of mouse weight; average weight is 26.4±6.1g, this shows that mouse weight was not centered on one location but instead had a fairly even distribution, especially around the mean weight
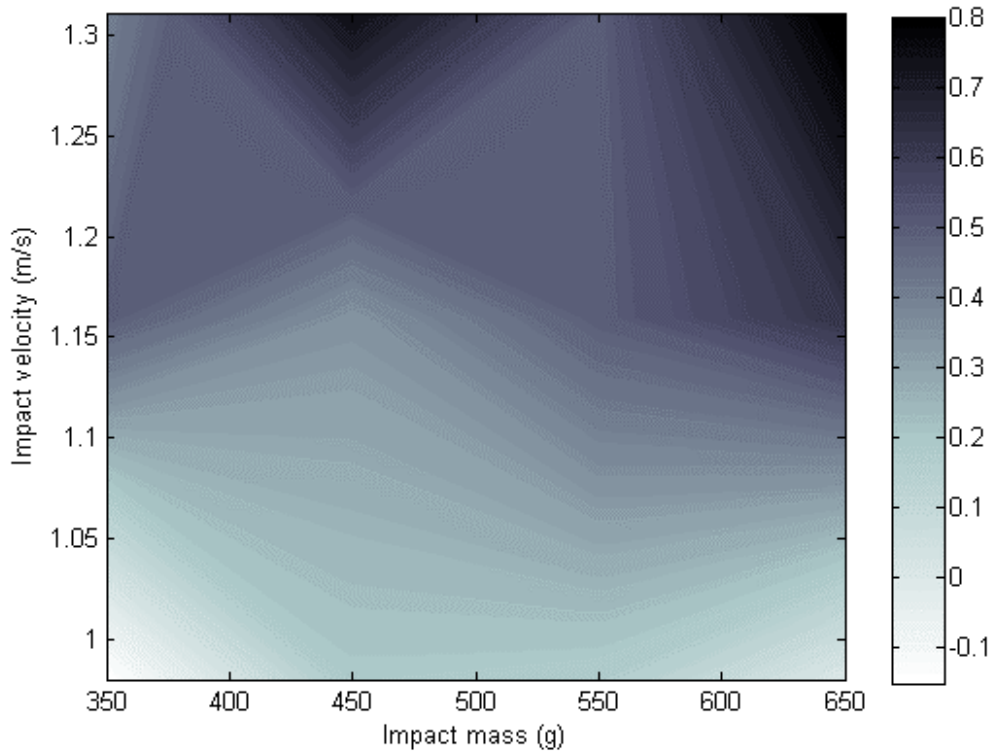
Figure 24: Contour plot of fracture types in Table 8; break-type range is (-1) = no break, (0) = transverse break, (1) = oblique/comminuted; plot shows that ideal kinetic energies for transverse fractures occurred at <1.05 m/s impact velocity and shows that impact velocity is more critical in determining break-type than impact mass

Modeling to predict fracture type

The fracture results in Table 8 were then imported into a statistical modeling
software package (SAS 9.1) for two purposes: to establish the best-fit modeling equation
using possible parameters of W, M, and V to predict break type, and to determine if any
of the above parameters are insignificant in order to simplify the modeling equation. In
total fifteen (15) model equations were applied, with the chosen modeling equation based
on significance (P-value) rather than root-mean-squared error or r-squared values due to
the nominal nature of the output (break-type, BT). These equations are provided in Table
9. Since Model #15 was ultimately chosen (for reasons provided in the Discussion
chapter), the equation and predicted contour plot of the 80% success zone are provided in
Figure 25.

Table 9: Model fits for break-type (BT) using parameters of mouse weight (*W*), impact mass (*M*) and impact velocity (*V*); significance of correlation to data of model and insignificant parameters are also provided, with "passing" equating to P<0.05

Model #	Mouse Group	Model Equation	Model P-Value	Pass/Fail	Insignificant Parameters	Pass/Fail
1	Small	$B.T. = \alpha + \chi W + \gamma M + \delta V$	0.2482	F	W, M, V	F
2	Small	$B.T. = \alpha + \chi W + \gamma M + \lambda V^2$	0.2305	F	W, M, V²	F
3	Small	$B.T. = \alpha + \chi W + \beta MV^2$	0.2030	F	W, MV²	F
4	Med	$B.T. = \alpha + \chi W + \gamma M + \delta V$	0.5051	F	W, M, V	F
5	Med	$B.T. = \alpha + \chi W + \gamma M + \lambda V^2$	0.5573	F	W, M, V²	F
6	Med	$B.T. = \alpha + \chi W + \beta MV^2$	0.7070	F	W, MV²	F
7	Large	$B.T. = \alpha + \chi W + \gamma M + \delta V$	0.1388	F	W, M, V	F
8	Large	$B.T. = \alpha + \chi W + \gamma M + \lambda V^2$	0.1446	F	W, M, V²	F
9	Large	$B.T. = \alpha + \chi W + \beta MV^2$	0.0285	P	W	F
10	All	$B.T. = \alpha + \chi W + \gamma M + \delta V$	<0.0001	P	W, M	F
11	All	$B.T. = \alpha + \chi W + \gamma M + \lambda V^2$	<0.0001	P	W, M	F
12	All	$B.T. = \alpha + \chi W + \delta V + \varepsilon M^2$	<0.0001	P	W, M²	F
13	All	$B.T. = \alpha + \chi W + \beta MV^2$	<0.0001	P	none	P
14	All	$B.T. = \alpha + \gamma M + \delta V$	<0.0001	P	M	F
15	All	$B.T. = \alpha + \beta MV^2$	<0.0001	P	none	P

The optimal fit-values of Model # 15 are provided below:

$$BT = -0.292 + (0.0010)MV^2$$

Where: $BT = \begin{bmatrix} -1 = \text{No break} \\ 0 = \text{Transverse} \\ 1 = \text{Comminuted / Oblique} \end{bmatrix}$

and *M* = impact mass in grams, *V* = impact velocity in m/s

$$BT = -0.292 + (0.0010)MV^2$$
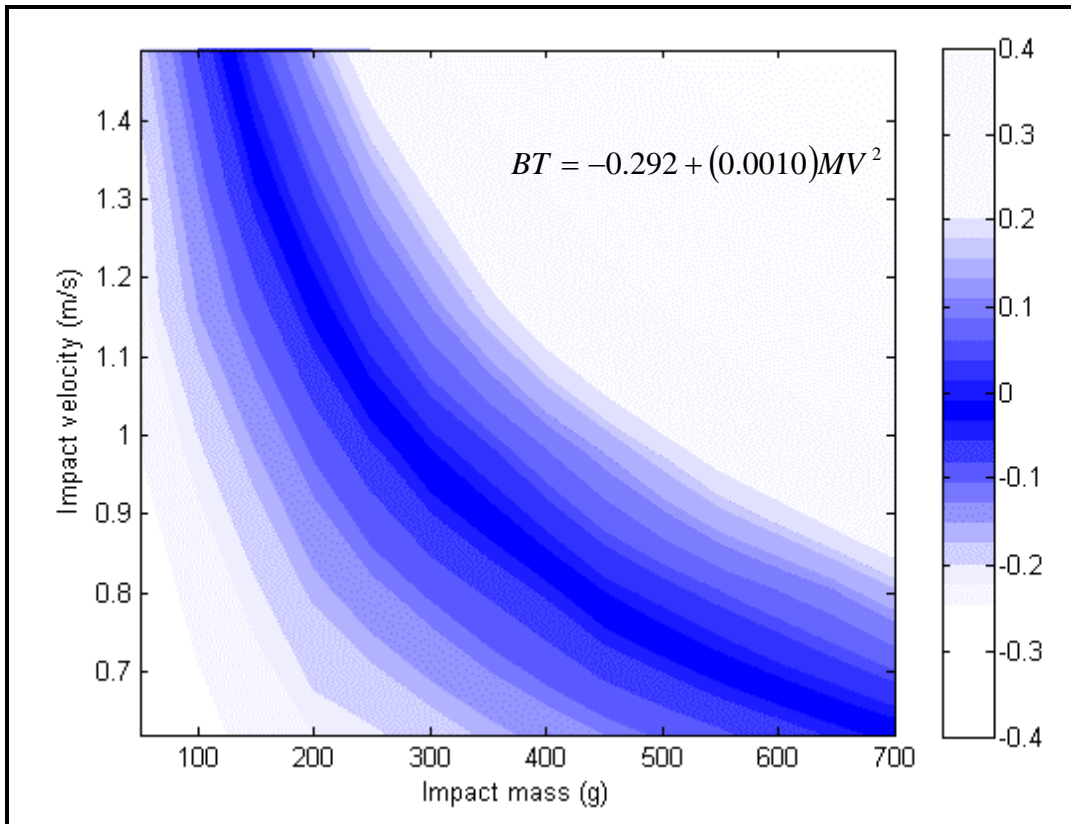
Figure 25: Predicted 80% success rate zone for transverse fractures based on Model #15; shaded area represents predicted 80% success zone and darkest area represents 95% success (BT=0), plot provides a visual representation of combinations of mass and velocity to use to obtain transverse fractures

7. ANALYSIS AND DISCUSSION

We have designed and assembled a fracture device to reproduce a murine transverse femur fracture. The device was able to control mass and velocity through the range of values described in Table 6, only required one user, and enabled proper placement of the mouse femur using the Mouse Positioning System. It was also equally adept at breaking either left or right femurs using the adjustable "half-pipe" torso bed. The relationships between M, V, W and BT were measured using the preliminary and comprehensive tests and their results are discussed below.

The preliminary testing results are displayed in Table 7 and show that the machine was able to create a range of fractures at the depth of 2mm, including transverse fractures with low kinetic energy (preliminary mouse #4) and oblique and comminuted fractures at higher levels of kinetic energy (preliminary mouse #7 and 9, respectively). Since no fractures were created with depth set at D_0, which was initially assumed to be correct, and because a range of fractures were created using D=2mm, this latter depth was used in the comprehensive fracture tests. The preliminary test was also in contradiction with Jackson's results (Jackson et al, 1970) which stated that the depth should be no more than D_0, the distance between top of anvils to intramedullary canal pin. A possible explanation for this difference may be that Jackson used a pneumatic device at 40 psi in a vertical position, which may have had a much higher kinetic energy than the levels used in this experiment. Therefore they could not afford to allow the striker to travel very far into the femur in order to avoid excessive application of energy.

The comprehensive testing results are provided in Table 8 and include the fracture results of the left and right femur for each mouse tested. The weight distributions are

provided below Table 8 in the histogram of Figure 23. The population density function in Figure 23 is relatively well distributed, especially around the mean and standard deviation of the population at 26.4 ± 6.1g. Since the frequency of weights was considered to be evenly distributed around this range, the significance of mouse weight in determining fracture type can be found for mice in the range. For example, this would not have been the case if every mouse weighed 22.0 grams, because mouse weight would have been a constant and therefore it would have been impossible to determine if the weight of the mouse had an effect on resultant break type for a given kinetic energy. The significance of mouse weight will be important for development of a modeling equation.

The contour plot in Figure 24 is a graphical representation of the break types from Table 8 and is irrespective of mouse weight. The graph primarily shows the heightened power of increasing impact velocity compared to increasing impact mass. As predicted with the theory of stress waves (Mott, 1948), increasing the velocity by only 25% greatly increases the chance of comminuted or oblique fracture. Using a quantitative break-type scale with -1 as no fracture, 0 as transverse and 1 as comminuted/oblique fracture, Figure 24 shows an increase of "break-type" by 0.45 for an increase of 25% velocity (1 m/s to 1.25 m/s). In contrast, increasing the mass by even 85% at a given velocity does not increase break type scale in most cases (350g to 650g, non-significant increase). This shows the power of the quadratic nature of kinetic energy at impact and how important it is to monitor velocity at impact in experimental bone fractures. These results indicated that the kinetic energy equation ($E_k = \frac{1}{2}MV^2$) may be an appropriate model to use for prediction of break type.

The next step was to take the data and attempt to develop a modeling equation to predict break type. The equation would have a combination of the parameters used in Table 8, including mouse weight (W), impact velocity (V) and impact mass (M). Several different linear and quadratic combinations of parameters were fit and are provided in Table 9. There are two important observations from the SAS results in this table. First, it is shown that modeling fits are not significantly coorelated ($P>>0.05$) to the data when three individual groups are used (Model #1-9), with the exception of model #9. However, the equations are significantly correlated when all data points are included, likely due to a higher sample number (n). In addition, mouse weight (W) was found to be an insignificant parameter in 12 out of the 13 cases when it was used. Therefore, based on these two observations, it was suggested that mouse weight (W) as a fit parameter has little affect in the range studied, provided that mouse weight was evenly distributed and not concentrated in a narrow range. As stated previously in this discussion, the histogram in Figure 23 shows fairly evenly distributed mouse weights, especially around the mean and first standard deviation. Thus it was concluded that for mice with weight 26.4±6.1g, mouse weight does not need to be taken into account for determination of output break type in the kinetic energy ranges tested (from Table 8).

Since mouse weight was found not to be significant, the next step was to determine what combination of impact mass and velocity would create the best fit. This was more difficult because of the nominal nature of the break type; root-mean-squared error (RMSE) or r-squared techniques are not applicable. Instead, the most optimal fit was determined first by significant correlation between the data and the equation as a whole, and then by the number of insignificant variables – ideally the equation should

have no insignificant variables for simplicity. From Table 9, two equations met these criteria, model #13 and 15. Since model #13 included mouse weight as a parameter which was concluded to be insignificant, model #15 was chosen as the correct modeling equation. The original hypothesis of this experiment was that break type could be predicted based on kinetic energy. As Table 9 shows, this hypothesis was ultimately supported, as the equation of the form: $BT = \alpha + \beta MV^2$ provided the best overall fit without any insignificant parameters.

The specific modeling fit for predicting a transverse fracture (BT=0) is shown in Figure 25. This shaded area of this contour plot represents the predicted 80% success rate zone for creating a transverse fracture. Additionally, the darkest shaded area represents the predicted 95% success rate transverse fracture zone. It is important to note that this plot does not take into account mouse weight, and thus should only be considered for mouse populations with weight distributions close to 26.4±6.1g. Average weights not close to this value or with standard deviations that are much higher may not be applicable, as mouse weight may be a significant variable in those cases. However, for a weight distribution close to the one tested in this experiment, Figure 25 is very useful for quickly identifying the correct impact mass and velocity combination to obtain a transverse fracture with a greater than 80% success rate.

The developed prediction equation has an important application in existing fracture devices which may use only one weight but are uncertain of the correct impact velocity to obtain a consistent transverse fracture. It is also useful for future fracture devices, which can be designed using the kinetic energy levels in Figure 25.

8. CONCLUSIONS

The present study has proposed a new and innovative design to be considered with the standard fracture device originally proposed by Bonnarens and Einhorn (1984). Previous issues with this design, including poor reproducibility and difficult two-person operation, are minimized when using the recommended kinetic energy levels and proposed design. Using an electromagnet and linear bearing assembly for consistent one-user operation coupled with the mouse positioning system enable reproducible and precise kinetic energy application to the diaphysis of the femur.

In addition to the novel design, the new model equation to predict transverse break type and the resulting contour plot are very useful to researchers who are searching to reduce the probability of a poor experimental fracture and wasted mice. As long as a fracture device uses a dynamic, non-quasistatic impact and a weight distribution of mice close to that used in this study, the kinetic energy levels proposed in this paper will help reduce risk of a poor fracture result.

9. RECOMMENDATIONS

The number of fractured femurs (120) and mouse weight distribution (26.4±6.1g) were limited by time to test them. One recommendation to further the understanding of murine fracture mechanics is to therefore test more mice with different weight distributions. This will help either support or reject our conclusion that mouse weight is an insignificant variable for ranges greater than those tested in this study. Another limitation of our results was that the machine was designed with a minimum impact weight of 350g and minimum impact velocity of 0.98 m/s. A useful contribution to our results would be to extend the variables of kinetic energy below these minimum values to better define the lower limits. One final limitation was that the velocity at impact of the machine was assumed to be frictionless and was not measured using high-speed photography or any other method, therefore the velocities may not be exact. It would be useful to verify what the exact impact velocities are to be as precise as possible.

Researchers would also benefit from using either our design or our recommended kinetic energy levels in a live mouse study. Studying the bone growth on transgenic or other mice using the proposed machine and recommendations would result in a higher success rate of transverse fracture. Attempting to genetically modify mice or using drug treatments on mice with transverse fractures created by this device may also give insight into how bone healing may be expedited in humans.

REFERENCES

Anderson, T.L. (2005). *Fracture mechanics: Fundamentals and applications, third edition*. Boca Raton, FL: CRC Press.

Bonnarens, F. & Einhorn, T.A. (1984). Production of a Standard Closed Fracture in Laboratory Animal Bone. *Journal of Orthopaedic Research*. *2*, 97-101.

Boyan, B.D., Caplan , A.I., Heckman , J.D., Lennon, D.P., Ehler, W., & Schwartz, Z. (1999). Osteochondral progenitor cells in acute and chronic canine non-unions. *Journal of Orthopaedic Research*. *17*, 246-255.

Brainard, B.J., Slauterbeck, J., & Benjamin, J.B. (1992). Fracture patterns and mechanisms in pedestrian motor-vehicle trauma: the ipsilateral dyad. *Journal of Orthopaedic Trauma*. *6*, 279-282.

Cardany, C.R., Rodeheaver, G., Thacker, J., Edgerton, M.T., & Edlich, R.F. (1976).The crush injury: a high risk wound. *JACEP*. *5*, 965-970.

Carmouche et al, (2005).Lead exposure inhibits fracture healing and is associated with increased chondrogenesis, delay in cartilage mineralization and a decrease in osteoprogenitor frequency. *Envionmental Health Perspectives*. *113*, 749-755.

Griffith, A.A. (1920).The phenomenon of rupture and flow in solids. *Philosophical Transactions of the Royal Society of London*. *Ser. A., 221*, 163-198.

Jackson, R.W., Reed, C.A., Israel, J.A., Abou-Keer, F.K., & Gardside, H. (1970).Production of a standard experimental fracture. *Canadian Journal of Surgery*. *13*, 415-420

Lea, Tor (2006). Mesenchymal stem cell differentiation pathways. Retrieved February 24, 2007, from Norway Institute of Immunology Web site: http://www.stemcell.no/groups/Lea/lea.htm

Manigrasso, AuthorM.B., & O'Connor, J.P. (2004). Characterization of a closed femur fracture model in mice. *Journal of Orthopaedic Trauma*. *18 (10)*, 687-694.

Martin, R.B., Burr, D.B., & Sharkey, N.A. (1998). *Skeletal Tissue Mechanics*. New York: Springer.

McGee, A.M., Qureshi, A.A., & Porter, K.M. (2004). Review of the biomechanics and pattern of limb fractures. *Trauma*. *6*, 29-40.

Minguell, J.J., Erices, A., & Conget, P. (2001). Mesenchymal stem cells. *Experimental Biology and Medicine*. *226*, 507-520.

Mott, N.F. (1948).Fracture of metals: Theoretical considerations. *Engineering*. *165*, 16-18.

Nalla, R.K., Kinney, J.H., & Ritchie, R.O. (2003). Effect of orientation on the in vitro fracture toughness of dentin: the role of toughening mechanisms. *Biomaterials*. *24*, 3955-3968.

Ozkaya, N., & Nordin, M. (1999). *Fundamentals of biomechanics: Equilibrium, motion and deformation, second edition*.New York: Springer.

Perez, N. (2004). *Fracture mechanics*. New York: Kluwer Academic Publishers.

Snedeker, J.G., Barbezat, M., Niederer, P., Schmidlin, F.R. & Farshad, M. (2005).Strain energy density as a rupture criterion for the kidney: impact tests on porcine organs, finite element simulation and a baseline comparison between human and porcine tissues. *Journal of Biomechanics*. *38*, 993-1001.

Wirtz, D.C., Schiffers, N., Pandorf, T., Radermacher, K., Weichert, D. & Forst, R., (2000).Critical evaluation of known bone material properties to realize anisotropic FE-simulation of the proximal femur. *Journal of Biomechanics*. *33*, 1325-1330

Yaoita, H., Orimo, H., Shirai, Y. & Shimada, T. (2000).Expression of bone morphogenetic proteins and rat distal-less homolog genes following rat femoral fracture. *Journal of Bone and Mineral Metabolism*. *18*, 63-70.

GLOSSARY

129/SvEv – a wild-type strain of mice known for their small size and easy maintenance

Accuracy – achieving correct break type

Anvil – the two support pieces underneath the femur that act as stable bases to support three-point bending

Comminuted fracture – a straight or deviatory fracture that divides into small fragments on the opposite side of fracture initiation

D – depth of blade deflection, measured from the top surface of the anvil to the lowest point that the blade travels; D_0 is the distance from the intramedullary canal pin to the anvil top surface

G – gap distance between the top anvil surfaces; the effective length of the three-point bending

Intramedullary canal pin – a stainless steel 30-gauge pin inserted into the mouse femur pre-fracture to fixate the fractured bone segments and ensure bony union in the healing process

M – mass of shaft, blade, thumbwheel, anti-rotation pin, magnets and additional weights

MPS – "Mouse Positioning System," the novel mouse femur and body orientation components proposed in this paper

MSCs – "Mesenchymal Stem Cells," the progenitor cells responsible for the proliferation of osteocytes in response to stimuli

Murine – mouse

Oblique fracture – a straight break that deviates more than 30° from the minor axis of the bone

Osteocytes – the primary cells of bone

Osteogenesis – the process of building bone through packing of osteocytes in specific, predetermined orientations based on lines of principal stress

Precision – reproducible, but not necessarily the desired result

Spiral fracture – a helical shaped break along the major axis of the bone

Soft tissue damage – the process of physically damaging cells, blood vessels and surrounding muscle/dermal tissue from an impact that induces an inflammatory/repair response with MSCs

Striker – the impacting unit in a three-point bending drop test, used to apply kinetic energy and fracture the specimen

Three-point bending – the mechanical test of suspending a specimen in the air, supporting its two ends and subsequently applying a load in the middle to cause fracture; load may be quasistatic for force or dynamic in kinetic energy

Transgenic – a genetically modified organism often used in mouse models to test for gene function

Transverse fracture – a straight, closed break across the minor axis of the bone that does not diverge more than 30°; permits easiest measure of osteogenesis

V – velocity of blade at impact with femur, measured from the known height of shaft drop and assumed to have frictionless descent

W – weight of mouse, in grams

APPENDICES

Table A1: Gravity-driven prototype designs

Design Constraints			Uniaxial		Pendulum		Incline Plane	
Cannot cost more than $2450			Y		Y		Y	
Right leg only			Y		Y		Y	
Non-Invasive			Y		Y		Y	
Smaller than 3 cubic feet			Y		Y		Y	
Non-Comminuted			Y		Y		Y	
Design Objectives	Weight (%)	Score	Weighted Score	Score	Weighted Score	Score	Weighted Score	
Closed, transverse fracture in middle 1/3 of femur	30	0.8	24	0.7	21	0.3	9	
Reproducible fracture	25	0.75	18.75	0.7	17.5	0.4	10	
Single person for operation	5	1	5	1	5	1	5	
Simple design	15	0.95	14.25	0.6	9	0.8	12	
Accommodation for different sizes of mice	5	1	5	1	5	1	5	
Adjustable variables of kinematics	10	1	10	1	10	1	10	
High energy impact fracture	10	1	10	1	10	1	10	
TOTAL:	100		**87**		**77.5**		**61**	

Table A2: Selection matrix of mouse torso stabilization methods

Design Constraints			Flat table		Mold		Half pipe		Inclined plane	
Material compatible with cleaning			Y		Y		Y		Y	
Non-Invasive			Y		Y		Y		Y	
Fits on MPS bed without obstructing device			Y		Y		Y		Y	
Holds body in desired position			Y		Y		Y		Y	
Low cost			Y		Y		Y		Y	
Design Objectives	Weight (%)	Score	Weighted Score	Score	Weighted Score	Score	Weighted Score	Score	Weighted Score	
User friendly	20	0.6	12	0.8	16	0.8	16	0.7	14	
Holds mouse securely	20	0.8	16	0.8	16	0.9	18	0.5	10	
Single person for operation	15	0.9	13.5	0.8	12	0.8	12	0.7	10.5	
Simple design	15	0.6	9	0.7	10.5	0.8	12	0.8	12	
Accommodation for different sizes of mice	15	0.8	12	0.5	7.5	0.8	12	0.8	12	
Adjustable	15	0.8	12	0.5	7.5	0.8	12	0.5	7.5	
TOTAL:	100		74.5		69.5		**82**		66	

Table A3: Functions-means chart for gravity driven designs

Functions	Gravity-Driven	Pneumatic	Electromagnet	Cam
Device should hold femur in proper anatomical position for precision and accuracy	femur held horizontally with notches in the anvils to hold femur in place	femur held horizontally manually positioned on table	femur held horizontally with straps on the support anvils	femur is held vertically with straps
Holds mouse body in supine position	pins and straps on table holds mouse body in supine postion	angle-adjustable table to support mouse body while fracture is created	additional straps to hold the body in place	mouse held with straps in a vertical position
Creates a fracture	uniaxial gravity-driven weight drop generates KE adjustable mass/stop height	air pressure with regulator resettable with spring and exhaust vent	solenoid strikes femur vertically from beneath w/ adjustable current	electric motor drives a wheel with a horizontal arm through columns

Table A4: Pairwise comparison chart based on client needs for design considerations

	Accuracy	Precision	Reliability	Cost	Safety	User-Friendly	Durability	TOTALS
Accuracy		0	1	1	1	1	1	5.0
Precision	1		0.5	1	1	1	1	5.5
Reliability	0	0.5		1	1	1	1	4.5
Cost	0	0	0		0	0	1	1.0
Safety	0	0	0	1		1	1	3.0
User-Friendly	0	0	0	1	0		1	2.0
Durability	0	0	0	0	0	0		0.0
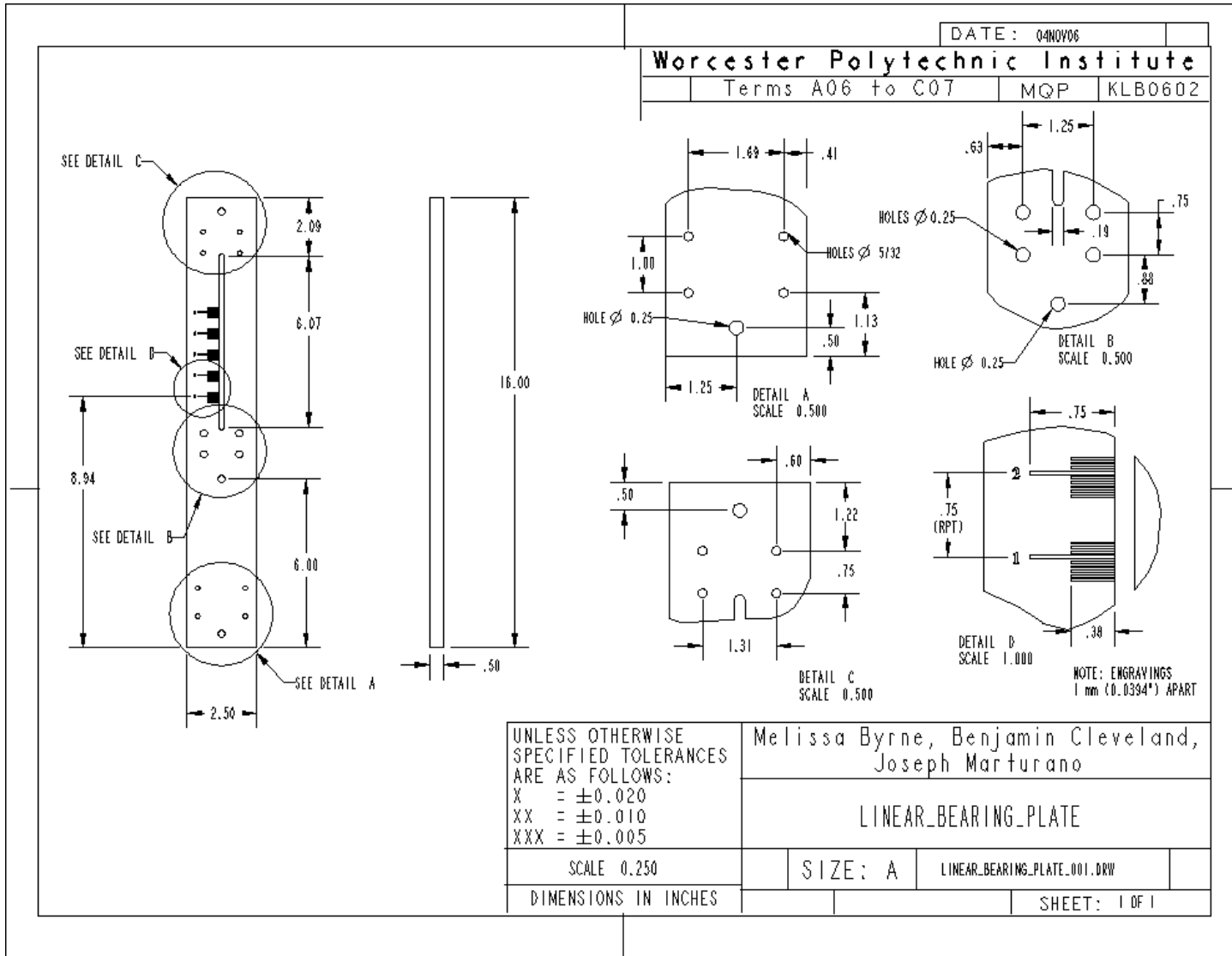
Figure A1: Detail drawing of linear bearing plate showing placement of linear bearings, stop block and height indicators; material: aluminum

Worcester Polytechnic Institute

Terms A06 to C07 | MQP | KLB0602

8.50

ARC PATH 60° CENTERED

1.25

4.00

R2.02 R1.74

1.63

DETAIL A
SCALE 1.000

0.25 Ø

.1875

NOTE: ARCS HAVE
RADII LISTED ABOVE,
REFERENCE IS CENTER
OF PLATE

3.75

4.75

.62

.375

SEE DETAIL A

UNLESS OTHERWISE
SPECIFIED TOLERANCES
ARE AS FOLLOWS:
X   = ±0.020
XX = ±0.010
XXX = ±0.005

Melissa Byrne, Benjamin Cleveland,
Joseph Marturano

MPS_FLOATING_BASE_PLATE

SCALE 0.500

SIZE: A | MPS_FLOATING_BASE_PLATE_001.drw

DIMENSIONS IN INCHES

SHEET: 1 OF 1

ALL HOLES 1/4" Ø

65

Figure A2: Detail drawing of adjustable height MPS plate; arc centered around hole closest to arc; material: aluminum

Figure 26: Detail drawing of anvil with notches for femur; material: 316 stainless steel

Table A5: Prototype cost and parts list

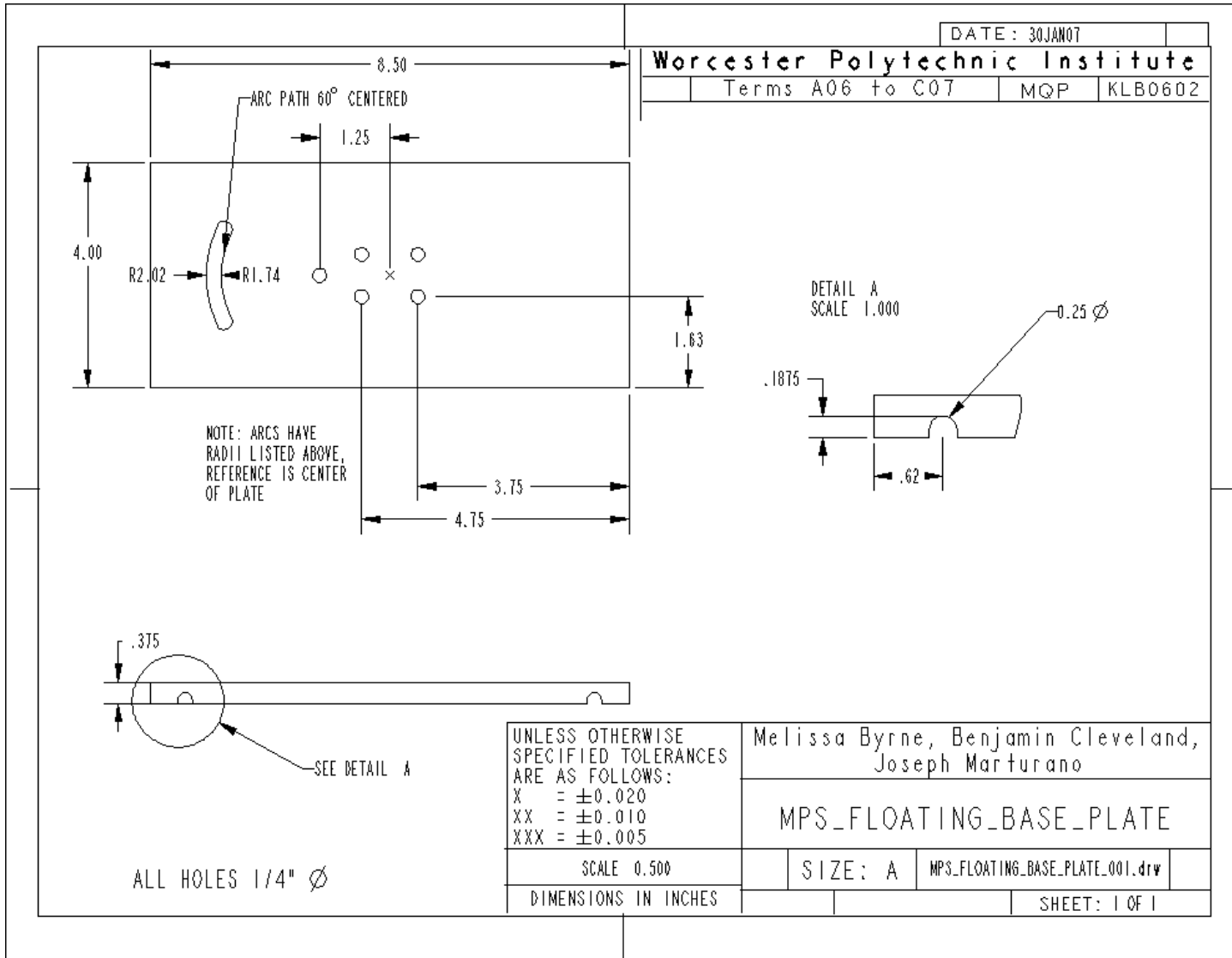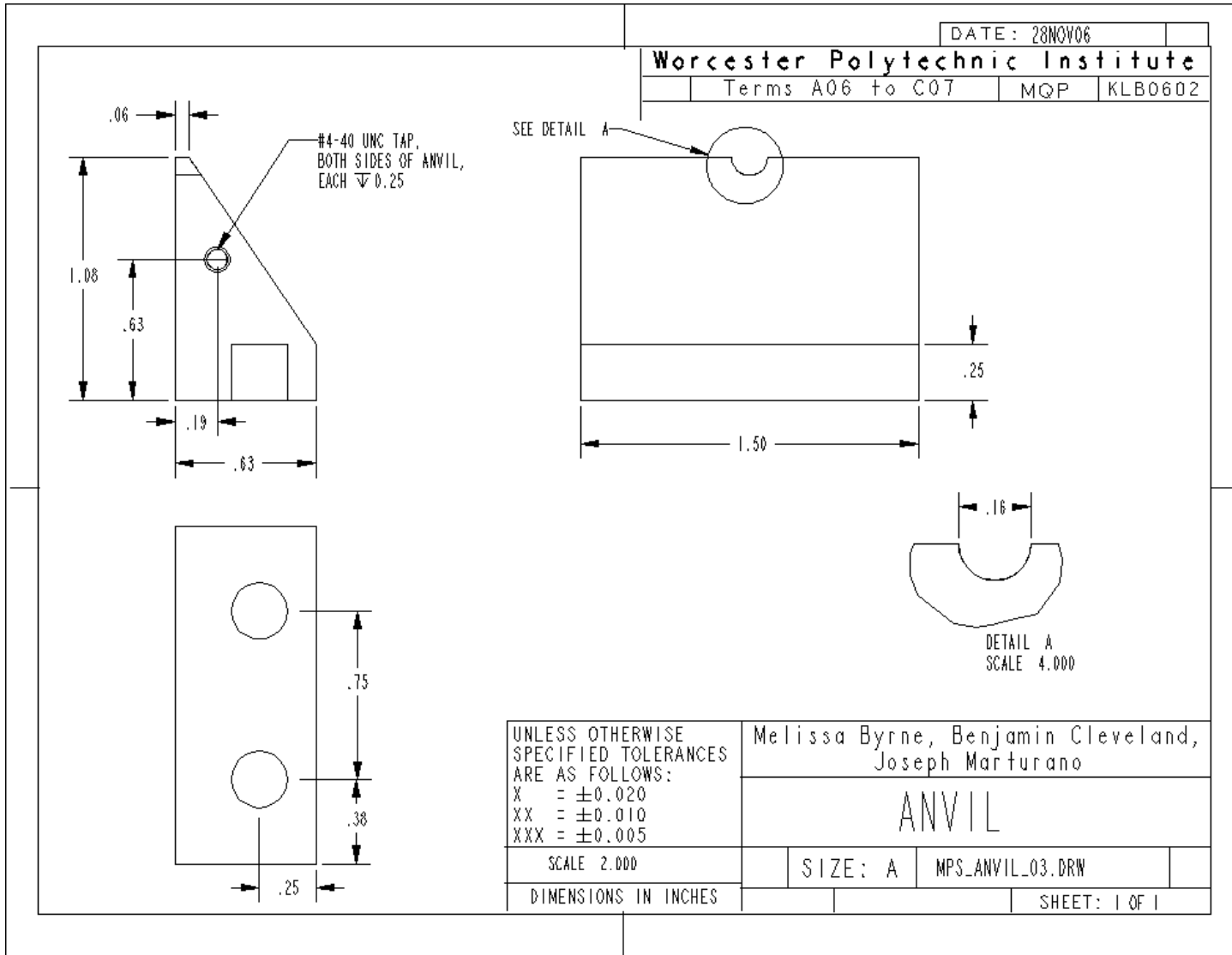| Vendor	Description	Price Each	Qty	Line Cost
McMaster-Carr	Foot Switch	$ 10.53	1	$ 10.53
McMaster-Carr	Lower Shaft	$ 66.15	1	$ 66.15
McMaster-Carr	Upper Shaft	$ 26.03	1	$ 26.03
McMaster-Carr	80lb Electromagnet	$ 48.60	1	$ 48.60
McMaster-Carr	Neogymium Ring Magnet	$ 28.29	4	$ 113.16
McMaster-Carr	AL 0.75x2x3"	$ 33.68	1	$ 33.68
McMaster-Carr	AL 0.75x2x1"	$ 14.48	1	$ 14.48
McMaster-Carr	AL 0.75x12x12"	$ 71.38	1	$ 71.38
McMaster-Carr	AL 0.50x2.50x3"	$ 63.19	1	$ 63.19
McMaster-Carr	AL 0.25x1x12"	$ 13.76	1	$ 13.76
McMaster-Carr	AL 0.75x4x36"	$ 59.28	1	$ 59.28
McMaster-Carr	SS 0.75x1.50x12"	$ 58.33	1	$ 58.33
McMaster-Carr	SS Thumbwheel	$ 6.08	2	$ 12.16
McMaster-Carr	1/4" Linear Bearing	$ 31.40	1	$ 31.40
McMaster-Carr	1/2" Linear Bearing	$ 55.68	1	$ 55.68
McMaster-Carr	AL 0.375x4x1"	$ 13.04	1	$ 13.04
McMaster-Carr	AL 0.50x1.25x36	$ 15.32	1	$ 15.32
Hometech.com	400mA Power Supply	$ 10.95	1	$ 10.95
McMaster-Carr	AL 1.50x1.50x12"	$ 21.58	1	$ 21.58
McMaster-Carr	180lb Electromagnet	$ 49.75	1	$ 49.75
McMaster-Carr	16g Wire (25ft)	$ 4.93	1	$ 4.93
McMaster-Carr	SS Cap Screw Pack (10pk)	$ 7.23	1	$ 7.23
McMaster-Carr	AL 0.005x6x24"	$ 4.19	1	$ 4.19
McMaster-Carr	AL 0.003x6x24"	$ 3.97	1	$ 3.97
McMaster-Carr	MS Cap Screw Pack (10pk)	$ 3.38	1	$ 3.38
McMaster-Carr	Bronze Nut	$ 20.85	1	$ 20.85
Sealevel.com	500mA Power Supply	$ 12.95	1	$ 12.95
McMaster-Carr	SS 0.024x12x12"	$ 11.71	1	$ 11.71
McMaster-Carr	SS 0.030x12x12"	$ 12.29	1	$ 12.29
McMaster-Carr	SS 1.50" Pipe	$ 18.53	1	$ 18.53
McMaster-Carr	AL 1/8" Rod, 12" L	$ 4.00	1	$ 4.00
Home Depot	1.5"D PVC Pipe, 18"L	$ 2.00	1	$ 2.00
Home Depot	2.0"D PVC Pipe, 18"L	$ 2.69	1	$ 2.69
Home Depot	3/4" Rubber Bumpers	$ 2.28	1	$ 2.28

Table A3: Prototype cost and parts list (cont.)

Vendor	Description	Price Each	Qty	Line Cost
Home Depot	1/4"-20 Wingnuts (4pk)	$ 0.79	1	$ 0.79
Radioshack	Orange LED w/Holder	$ 1.99	1	$ 1.99
Lowe's	Hex 1/4"-20 X3"	$ 1.12	1	$ 1.12
Lowe's	Hex 1/4"-20 X1"	$ 2.23	2	$ 4.46
Lowe's	Hex 1/4"-20 X2"	$ 1.42	2	$ 2.84
Home Depot	6-32 X 1.25" Bolt/Nuts	$ 0.90	1	$ 0.90
Home Depot	1/8" X 1" Washers	$ 0.79	1	$ 0.79
Home Depot	Hex 1/4"-20 1" Bolt	$ 0.09	2	$ 0.18
Home Depot	Hex 1/4"-20 2.5" Bolt	$ 0.15	4	$ 0.60
Home Depot	Hex 1/4"-20 3" Bolt	$ 0.17	5	$ 0.85
McMaster-Carr	Control Box 3.25"	$ 2.86	1	$ 2.86
McMaster-Carr	Toggle Switch	$ 3.48	1	$ 3.48
McMaster-Carr	Hex 1/4"-20 7" Bolt	$ 4.70	1	$ 4.70
McMaster-Carr	16g Wire (25ft)	$ 4.93	1	$ 4.93
McMaster-Carr	Hex 1/4"-20 5/8" (10pk)	$ 4.69	1	$ 4.69
McMaster-Carr	Hex 1/4"-20 7" Bolt	$ 4.70	2	$ 9.40
McMaster-Carr	Iron handle 1/4"-20	$ 2.24	1	$ 2.24
Troemner	Brass slotted weight, 20g	$ 7.35	2	$ 14.70
Troemner	Brass slotted weight, 50g	$ 8.40	1	$ 8.40
Troemner	Brass slotted weight, 100g	$ 9.45	3	$ 28.35
McMaster-Carr	Locknut 1/4"-20	$ 1.69	4	$ 6.76
McMaster-Carr	Knurled Nut 1/4"-20	$ 5.40	1	$ 5.40
McMaster-Carr	SS 4-40 Screw 1/4" L (50pk)	$ 5.04	1	$ 5.04
Home Depot	Hex 1/4"-20 4" Fully Threaded (2pk)	$ 3.99	1	$ 3.99
Home Depot	Misc. Hardware Packet	$ 0.98	1	$ 0.98
Home Depot	Hex 1/4"-20 3" Bolt	$ 0.17	1	$ 0.17
Home Depot	Misc. Hardware Packet	$ 0.98	1	$ 0.98
Home Depot	Misc. Hardware Packet	$ 0.98	1	$ 0.98
Home Depot	Socket Screw 1/4" (2pk)	$ 0.74	1	$ 0.74
Home Depot	Socket Screw 1/2" (2pk)	$ 0.72	1	$ 0.72
Home Depot	Hex 1/4"-20 5 1/2" Bolt	$ 0.32	2	$ 0.64
Home Depot	Hex 1/4"-20 5" Bolt	$ 0.60	2	$ 1.20
Home Depot	1/4" ID 1" OD Fender Washer	$ 0.13	8	$ 1.04
Home Depot	#6 Lock Washer Split (30pk)	$ 0.98	1	$ 0.98
Home Depot	#6 Lock Washer Tooth (20pk)	$ 0.98	1	$ 0.98

Total Shipping and Handling Cost: $89.76

Total Prototype Cost: $1,118.08